Antifragile perimeter control

Anticipating and gaining from disruptions with reinforcement learning

Author(s):
Sun, Linghang; Makridis, Michail; Genser, Alexander; Axenie, Cristian; Grossi, Margherita; Kouvelas, Anastasios

Publication date:
2024-02-20

Permanent link:
https://doi.org/10.3929/ethz-b-000661353

Originally published in:
arXiv, https://doi.org/10.48550/ARXIV.2402.12665

Antifragile Perimeter Control: Anticipating and Gaining from Disruptions with Reinforcement Learning

Linghang Sun[a,*], Michail A. Makridis[a,*], Alexander Genser[a], Cristian Axenie[b], Margherita Grossi[c], Anastasios Kouvelas[a]

[a]*Institute for Transport Planning and Systems, ETH Zurich, Zurich, 8093, Switzerland*
[b]*Computer Science Department and Center for Artificial Intelligence, Technische Hochschule Nürnberg, Nürnberg, 90489, Germany*
[c]*Intelligent Cloud Technologies Lab, Huawei Munich Research Center, Munich, 80992, Germany*

Abstract

The optimal operation of transportation networks is often susceptible to unexpected disruptions, such as traffic incidents and social events. Many established control strategies rely on mathematical models that struggle to cope with real-world uncertainties, leading to a significant decline in effectiveness when faced with substantial disruptions. While previous research works have dedicated efforts to improving the robustness or resilience of transportation systems against disruptions, this paper applies the cutting-edge concept of *antifragility* to better design a traffic control strategy for urban road networks. Antifragility sets itself apart from robustness and resilience as it represents a system's ability to not only withstand stressors, shocks, and volatility but also thrive and enhance performance in the presence of such adversarial events. Hence, modern transportation systems call for solutions that are antifragile. In this work, we propose a model-free deep Reinforcement Learning (RL) scheme to control a two-region urban traffic perimeter network. The system exploits the learning capability of RL under disruptions to achieve antifragility. By monitoring the *change rate* and *curvature* of the traffic state with the RL framework, the proposed algorithm anticipates imminent disruptions. An additional term is also integrated into the RL algorithm as *redundancy* to improve the performance under disruption scenarios. When compared to a state-of-the-art model predictive control approach and a state-of-the-art RL algorithm, our proposed method demonstrates two antifragility-related properties: (a) gradual performance improvement under disruptions of constant magnitude; and (b) increasingly superior performance under growing disruptions.

Keywords: Antifragility, Reinforcement Learning (RL), Perimeter control, Traffic disruptions, Macroscopic Fundamental Diagram (MFD)

1. Introduction

Transportation networks serve as vital channels for the movement of people and goods. The optimization of transportation systems has become a focal point for researchers, resulting in a multitude of research endeavors and practical implementations in the field of Intelligent Transportation Systems (ITS), as in Figueiredo et al. (2001); Haque et al. (2013). Given that various

*Corresponding author.
Email addresses: lisun@ethz.ch (Linghang Sun), mmakridis@ethz.ch (Michail A. Makridis)

sorts of unexpected events, such as traffic accidents, social events, unfavorable weather conditions, etc., often occur unexpectedly in real-world networks, examining the robustness and resilience of the transportation system is crucial in the research of ITS (Ganin et al., 2019).

With the ever-growing population in the cities and urbanization, traffic systems have gained both volume and complexity. According to the Federal Statistical Office of Switzerland, private motorized road traffic experienced a steady increase of 54% between 1980 and 2019 (Federal Statistical Office, 2020). The rise in traffic volume can lead to an escalation of intensified congestion and more traffic incidents (Chang and Xiang, 2003). Therefore, urban road networks need to secure a decent level of service even when confronted by various disruptions of unforeseen magnitudes. This also raises the question of whether the current levels of robustness and resilience in transportation systems are sufficient to handle such challenges.

To address such issues, *antifragility* has shed light on a feasible solution and provides a possible new evaluation criterium. First introduced in the bestseller *Antifragile: Things that Gain from Disorder* by Nassim Nicholas Taleb in 2012, it has then been mathematically explained in Taleb (2013); Taleb and Douady (2013), providing insights on designing systems that can benefit from disruptions and perform better under growing volatility and randomness. Since then, antifragility has gained significant interest from both the public and academia, particularly in the field of risk engineering (Aven, 2015). The potential of antifragility can also be leveraged within transportation systems to tackle the increasingly severe traffic problems and non-linear dynamics that modern cities face today.

However, how to design antifragile transportation systems remains unexplored. One promising approach to induce antifragility is by using learning-based algorithms. With the rapid advancement of big data and sensor techniques, using Machine Learning (ML), particularly Reinforcement Learning (RL)-based methods has also become a trending practice in designing traffic management and control strategies (Zhu et al., 2019; Haydari and Yılmaz, 2022). Through interacting with a given environment, an RL agent enhances its decision-making ability over time (Sutton and Barto, 2018). One advantage of RL over established controllers is that it allows for more flexibility and competence in dealing with multivariate nonlinearities in complex environments (Li, 2018; Mysore et al., 2021). RL agents can gradually adjust their decision-making when deployed to an environment subject to variations, whereas established controllers, such as PID controllers, may need intensive manual tuning of parameters. Also, additional information can be fed to the RL agent with ease as a representation of the environment, regardless of knowledge of the model dynamics. In contrast, structured model dynamics of the system are often required when designing a controller (Bemporad, 2006). This feature of RL can also be exploited to explore hidden information from the vast amount of data collected through various sensors. As a result, modern traffic control systems have the potential to acquire knowledge from traffic disruptions, respond preemptively with merely early signs, and exhibit increasingly better performance as disruptions escalate.

The main goal of this paper is to design an RL algorithm to empower traffic control strategies, i.e., perimeter control in this study, to be antifragile against volatility and randomness, which are instantiated through disruptions with various magnitudes and onsets. First, we distinguish the concept of antifragility as opposed to other more commonly used terms in the field of transportation, namely robustness and resilience. Then we introduce how antifragility can be induced by integrating derivatives (i.e., change rate and curvature of traffic state) and redundancy into the state space and reward function of an RL algorithm. We simulate perimeter control in a cordon-shaped urban road network, subject to demand and model disruptions. Based on the

simulation results, we propose a quantitative approach to evaluate and compare the antifragility property among different methods.

The key contributions of this work can be summarized as follows: This work is the first to embrace the concept of antifragility in the context of the daily operation of transportation systems. This study demonstrates the effectiveness of incorporating derivatives and redundancy to handle system disruptions. Also, the proposed antifragile model-free RL-based algorithm achieves better performance compared to both a model-based control strategy that requires a priori knowledge and another state-of-the-art model-free RL-based method.

2. Literature review

This section provides a review of the relevant literature with three topics covered in this work. First, a macroscopic traffic model and the control strategy applied in this paper are introduced, which serve as the basis of model dynamics for the simulation environment. Following that, since antifragility itself is a novel research topic and the link between RL and antifragility is yet absent, we present state-of-the-art research on leveraging RL algorithms to induce robustness and resilience of traffic control strategies. And eventually, based on the literature, we introduce antifragility conceptually and how an antifragile system can be designed.

Alleviating urban network congestion can be realized through various traffic control strategies. Since Daganzo (2007) proved the existence of the Macroscopic Fundamental Diagram (MFD) theoretically and Geroliminis and Daganzo (2008) demonstrated the presence of the MFD with empirical data, the relationship between traffic flow and density has been established through the aggregation of individual microscopic data points. This relationship has paved the way for the development of control strategies on a macroscopic level, enabling more computationally feasible real-time control strategies for large-scale networks (Knoop et al., 2012), such as perimeter control (Keyvan-Ekbatani et al., 2012; Geroliminis et al., 2013; Kouvelas et al., 2017; Yang et al., 2017), pricing (Zheng et al., 2012; Zheng and Geroliminis, 2016; Genser and Kouvelas, 2022) and route guidance (Yildirimoglu et al., 2015; Fu et al., 2022).

Perimeter control is among the strategies that have attracted immense attention and research. Real-world implementation as shown in Ambühl et al. (2018) also demonstrated its applicability as an effective approach to regulating urban traffic. By refraining the incoming vehicles from adjacent regions into a protected zone, the traffic density in the protected area remains below the critical density, so a satisfactory level of service can be upheld (Keyvan-Ekbatani et al., 2012). Geroliminis et al. (2013) proposed an optimal perimeter control method using Model Predictive Control (MPC) and proved its effectiveness compared to a greedy controller in a cordon-shaped network. One major issue with the previous works is the MFD heterogeneity. To tackle this challenge, a substantial amount of effort has been made in investigating the partitioning algorithms so that a well-defined MFD can be referred to for a certain sub-network (Ambühl et al., 2019; Saedi et al., 2020). However, MFDs in the real world can hardly be well-defined, as demonstrated in Ambühl et al. (2021) with loop detector data over a year. Wang et al. (2015) and Ji et al. (2015) also showed that adverse weather conditions and traffic incidents can alter the shape of the MFDs and even a recovery from the peak-hour congestion may lead to a hysteresis (Gayah and Daganzo, 2011). These phenomena could potentially violate the mathematical model that serves as the foundation for the established model-based perimeter controllers.

To tackle the parameter uncertainties in the models caused by real-world disruptions, recent years have also witnessed a growing trend towards utilizing non-parametric learning-based

approaches in traffic control (Nguyen et al., 2018). Among different ML algorithms, RL has been researched extensively in transportation operations, e.g., traffic light control (Wei et al., 2019; Chen et al., 2020), dynamic pricing (Wang et al., 2022), delay management (Zhu et al., 2021). Particularly for perimeter control, recent works from Ni and Cassidy (2019) and Zhou and Gayah (2021) have illustrated the capability of RL algorithms to achieve similar or even superior performance compared to the established control methods.

Before introducing antifragility, two associated terms *robustness* and *resilience* commonly used in evaluating traffic control strategies and how they can be induced with RL are introduced. As Tang et al. (2020) mentioned, these terms are sometimes used interchangeably in transportation research works. Therefore, we follow the principles proposed by Zhou et al. (2019), that robustness is concerned with assessing a system's capacity to preserve its initial state and resist performance deterioration in the presence of uncertainty and disturbances, while resilience stresses the ability and speed of a system to recover from major disruptions to the original state. While researchers have endeavored to produce review articles in either the applications of RL in transportation (Haydari and Yılmaz, 2022; Haghighat et al., 2020) or robustness/resilience in transportation systems (Zhou et al., 2019; Tamvakis and Xenidis, 2012), a summarization of using RL algorithms in transportation to achieve robust or resilient urban networks remains absent. Here we briefly reviewed the existing studies that apply RL to regulate urban traffic that have demonstrated the robustness or resilience of their proposed methods. By transferring the knowledge of robust or resilient design, we can induce antifragility in our traffic control design through similar approaches. Table 1 shows a selection of papers around perimeter control and traffic signal control regulated with RL algorithms.

As can be seen, only two out of the ten papers are focused on the resilience of the RL-based traffic control strategies and the studied scenarios are traffic demand uncertainties and MFD errors (Zhou and Gayah, 2023) as well as lane closures (Korecki et al., 2023). When examining the system's robustness, the types of scenarios under consideration become more diverse, including incidents (Aslani et al., 2018; Rodrigues and Azevedo, 2019), sensor failures (Wu et al., 2020).

Table 1 also summarizes the RL setups to demonstrate the property of being either robust or resilient of each traffic control strategy. In these papers, some authors proved the superior robustness or resilience of their proposed methods directly through testing against the established methods as benchmarks, whereas others induced such properties by adding specific terms (italicized in Table 1) in the state space of the RL-algorithm. As a result, the algorithms are given additional information, potentially empowering the algorithms to anticipate ongoing disruptions. For instance, Rodrigues and Azevedo (2019) induced robustness by adding the elapsed time since the last green signal for each phase, Tan et al. (2020) experimented with speed or pressure (residual queue) as an additional state representation in the state space of the RL algorithm, Chu et al. (2020) supplemented the control policies of neighboring intersections as additional information to the agents, and Zhou and Gayah (2023) used an extra binary congestion indicator in the state space. The analysis of the state-of-the-art RL studies considers reversals or sudden changes in the state-action-reward dynamics, which evokes unanticipated uncertainty. The problem in these contexts is often to respond to unexpected results appropriately since they might indicate a shift in the environment. In this case, exploration refers to the process of looking for new information to improve the RL agent's understanding of the traffic dynamics under disruptions, which would then be used to identify better courses of action.

Ever since the concept of antifragility was proposed, it has become an increasingly popular concept in many disciplines, such as economy (Manso et al., 2020), biology (Kim et al., 2020),

Table 1: Traffic control strategies using RL with demonstrated robustness or resilience

Literature	Category	Objective	Scenarios	Robust	Resilient	Benchmark	RL method	State	Action	Reward
Zhou and Gayah (2021)	Perimeter control	Maximize trip completion under uncertainties	Demand and MFD uncertainties	Tested		No-control, MPC	DDPG	No. of vehicles, traffic demand	Perimeter control variables	Trip completion
Chen et al. (2022)	Perimeter control	Minimize total time spent under uncertainties/disturbances	Demand uncertainties, demand surge	Tested		MPC	AC-IRL	No. of vehicles	Perimeter control variables	Divergence from critical accumulation
Su et al. (2023)	Perimeter control	Maximize trip completion under uncertainties	Demand uncertainties	Tested		FT/Webster/ MP + PI	DQN	Flow, density, speed	Perimeter control variables	Ratio of flow over max flow
Zhou and Gayah (2023)	Perimeter control	Maximize trip completion under uncertainties and errors	Demand and MFD uncertainties		Induced[1]	No-control, MPC	MADDPG	No. of vehicles, traffic demand, *congestion indicator*	Perimeter control variables	Trip completion
Aslani et al. (2018)	Traffic signal control	Minimize average travel time under disturbances	Incidents, sensor noise	Tested		Cross comparison	DQN, AC, SARSA	Phase, pressure	Green time duration	Queue length
Chu et al. (2020)	Traffic signal control	Minimize queue length and delay, maximize vehicle speed and trip completion under demand uncertainties	Demand uncertainties, demand surge	Induced		IA2C, IQL-LR, IQL-DNN	MAA2C	Total delay, no. of vehicles, *adjacent info*	Signal configuration	Queue length, total delay
Rodrigues and Azevedo (2019)	Traffic signal control	Minimize total travel time, total delay, and total stop time	Demand surge, incidents, sensor failures	Induced		Self-comparison	DDQN	Queue length, *elapsed time in each phase*	Time extension, phase selection	Numerical derivative of queue length
Tan et al. (2020)	Traffic signal control	Minimize queue length at the intersection under uncertainties	Demand uncertainties	Induced		Self-comparison	DDQN	phase info, queue length, *speed, pressure*	Phase configuration	Queue length, duration over detection
Wu et al. (2020)	Traffic signal control	Minimize average vehicle delay under different scenarios	Demand uncertainties, sensor noise	Tested		Fixed-time, actuated	DDQN	No. of vehicles, phase, elapsed time, neighbor phases	No-change/ extend/ terminate	Queue length
Korecki et al. (2023)	Traffic signal control	Minimize average travel time under disruptions	Lane closure		Tested	Random, cyclical, demand, analytical+	DQN, DQN + heuristic	Vehicle occupancies	Green time duration	Negative pressure

Tested/Induced: Tested means the robustness or resilience is demonstrated through direct testing against other benchmark methods, without identifying which component in the RL algorithm results in such properties. Induced means the author identified that adding certain terms in the RL algorithm improves the robustness or resilience.
Italicized terms represent the additional information the authors applied as effective to design a robust/resilient system.

medicine (Axenie et al., 2022), and robotics (Axenie and Saveriano, 2023). However, current studies on antifragility in the field of engineering mostly pertain to post-disaster reconstruction efforts (Fang and Sansavini, 2017; Priyadarshini et al., 2022). Leveraging the potential of antifragility for the daily operations and optimization of transportation systems is a new and unexplored notion.

In Taleb (2012), in which the concept of antifragility was first introduced, two different levels of antifragility have been indicated: proto-antifragility and antifragility. To differentiate these two terms more clearly, we rename the latter as progressive antifragility. In contrast to robustness or resilience, proto-antifragility describes systems that can improve performance from experiencing disruptions, within a certain magnitude. A very illustrated example can be the biological process of hormesis. In this sense, proto-antifragility resembles adaptiveness, research works such as Fang and Sansavini (2017) are related to proto-antifragility of infrastructure under hazardous events. The higher level of antifragility, i.e., the progressive antifragility, lays emphasis on the concave response of the system regarding an increasing magnitude of disruptions. Its antonym, fragility, refers to systems that suffer from exponentially growing loss when faced with linearly increasing disruptions (Taleb and Douady, 2013), which is characterized by convexity and can be mathematically formulated with Jensen's inequality $E[g(X)] \geq g(E[X])$. On the contrary, the nonlinear relationship between external stressors and responses for antifragile systems is concave with $E[g(X)] \leq g(E[X])$. A system exhibiting proto-antifragility is not necessarily progressive antifragile at the same time.

Researchers have also proposed methods to incentive antifragile property of a system by emphasizing the derivatives to capture the temporal evolution patterns of the system dynamics, i.e., how fast the system state deviates towards a possible black swan event, and the curvature of this deviation (Taleb and Douady, 2013; Taleb and West, 2023; Axenie et al., 2022). With this additional information, the system can anticipate ongoing disruptions and be more responsive to drastic changes. Similar to the function of redundancy in resilience (Tan et al., 2019; Kamalahmadi et al., 2022), redundancy can also be added in the system to induce antifragility de Bruijn et al. (2020); Johnson and Gheorghe (2013); Munoz et al. (2022). Other feasible approaches also include time-scale separation and attractor dynamics (Axenie et al., 2022; Axenie, 2022).

3. Problem Formulation

This paper studies the problem of perimeter control between two homogeneous regions. A cordon-shaped urban network is investigated as in Geroliminis et al. (2013); Zhou and Gayah (2021), with the inner region representing a city center, as shown in Figure 1(a). Traffic demand for an Origin-Destination (OD) pair from region i to region j at time t is denoted as $q_{ij}(t)$. The inner and outer regions have different MFDs due to the difference in capacity to accommodate vehicles in the road networks within the city center and the surrounding region, defined as $G_i(n_i(t))$ as illustrated in Figure 1(b). Given the total number of vehicles with presence in region i at time t, denoted as $n_i(t)$, the total trip completion rate for this region i, denoted as $M_i(t)$, can be determined using the corresponding MFD, which comprises both the intraregional trip completion, i.e., $M_{ii}(t)$ and the interregional transfer flow, i.e., $M_{ij}(t)$ $(i \neq j)$ with $i, j \in \{1, 2\}$. In order to protect both regions from being overflown by possible high traffic demand, the percentage of the transfer flow allowed to go across the region perimeter at time t is regulated by two perimeter controllers denoted as $u_{ij}(t)$ $(i \neq j)$. A list of all notations used in this paper, including the notations used in defining the RL algorithm and the antifragile terms, is summarized in Table 2.

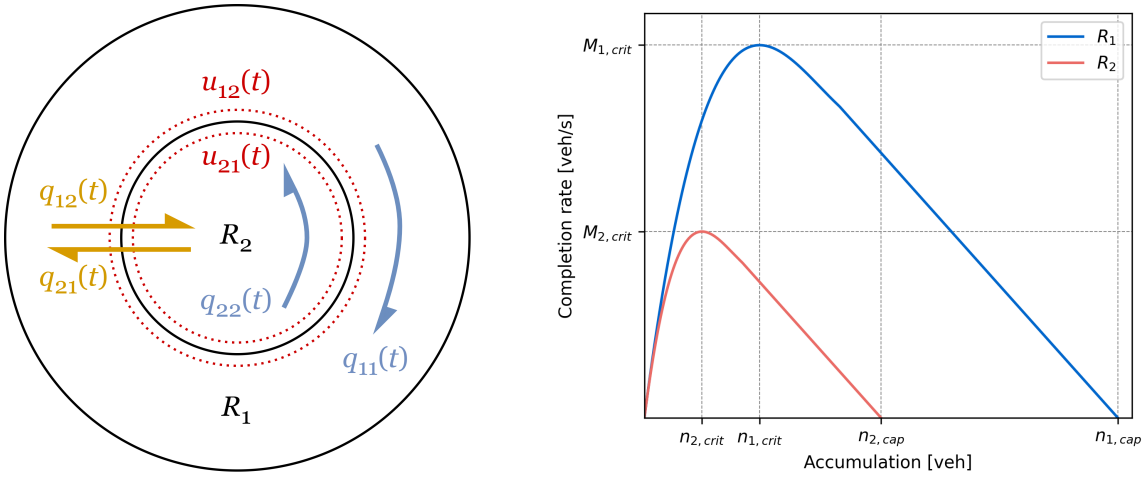

(a) The cordon-shaped urban network

(b) MFDs for the inner and outer regions.

Figure 1: The network structure and the related MFDs.

Eq. 1 describes the change rate of the intraregional vehicle accumulation of region i. It is the sum of intraregional traffic demand in this region, denoted as $q_{ii}(t)$, together with the perimeter control regulated transfer flow from region j to region i, defined as $u_{ji}(t) \cdot M_{ji}(t)$, then deducted by the trip completion within region i, denoted as $M_{ii}(t)$. Likewise, the change rate of interregional traffic accumulation, as in Eq. 2 shows, is the difference between the interregional traffic demand, denoted as $q_{ij}(t)$, and the regulated transfer flow $u_{ij}(t) \cdot M_{ij}(t)$:

$$\frac{dn_{ii}(t)}{dt} = q_{ii}(t) + u_{ji}(t) \cdot M_{ji}(t) - M_{ii}(t) \tag{1}$$

$$\frac{dn_{ij}(t)}{dt} = q_{ij}(t) - u_{ij}(t) \cdot M_{ij}(t), \ (i \neq j) \tag{2}$$

The total trip completion, i.e., $M_i(t)$ for region i at time t is calculated based on the trip accumulation and the related MFD, defined as $G_i(n_i(t))$, and is the sum of the intraregional trip completion, i.e., $M_{ii}(t)$, in Eq. 3 and the interregional transfer flow, i.e., $M_{ij}(t)\,(i \neq j)$, in Eq. 4:

$$M_{ii}(t) = \frac{n_{ii}(t)}{n_i(t)} \cdot G_i(n_i(t)) \tag{3}$$

$$M_{ij}(t) = \frac{n_{ij}(t)}{n_i(t)} \cdot G_i(n_i(t)), \ (i \neq j) \tag{4}$$

$$n_i(t) = \sum_{j=1,2} n_{ij}(t) \tag{5}$$

The objective function is to maximize the throughput of this cordon-shaped network, which is the sum of the intraregional trip completion in both regions.

$$J = \max_{u_{ij}(t)} \int_0^{t_{\text{end}}} \sum_{i=1,2} M_{ii}(t) dt \tag{6}$$

subject to the following boundary conditions:

Table 2: List of notations

Symbol	Meaning
1. General notations in problem formulation	
t	Time
Δt	Time step
t_{end}	Total simulation time
$n_{ij}(t)$	Vehicle accumulation with OD from region i to j at time t
$n_i(t)$	Vehicle accumulation in region i at time t
$u_{ij}(t)$	Perimeter control variables regulating flow from region i to j at time t
$q_{ij}(t)$	Traffic demand with OD pair i and j at time t
$G_i(n_i(t))$	Sum of trip completion and transfer flow in region i at time t
$M_{ij}(t)$	Trip completion with OD from region i to j $(i \neq j)$ at time t
$n_{i,\text{cap}}(t)$	Maximal number of vehicles (jam accumulation) in region i at time t
$n_{i,\text{crit}}(t)$	Vehicle accumulation with highest completion rate in region i at time t
J	Objective function
2. Notations in reinforcement learning	
$\mathcal{S}$	State space, the whole set of states the RL agent can transition to
s_t	$s_t \in \mathcal{S}$, the observable state in simulation at time t
$\mathcal{A}$	Action space, the whole set of actions the RL agent can act out
a_t	$a_t \in \mathcal{A}$, the action taken in simulation at time t
$\mathcal{R}$	The reward function for the RL agent
r_t	$r_t = \mathcal{R}(s_t, a_t)$, the received reward with state s_t and action a_t at time t
γ	Discount factor to favor rewards in the near future
$Q(s(t), a(t))$	Expected long-term return for taking action $a(t)$ in state $s(t)$ at time t
θ^{μ}	Weight parameter of the deep neural network for the actor network
θ^{Q}	Weight parameter of the deep neural network for the critic network
y_i	Expected long-term return calculated with the target critic network
L	The loss of the critic network
ρ^{β}	All possible trajectories of s_t
I	The objective function for the actor-network
3. Notations for the additional antifragile terms applied in reinforcement learning	
$\epsilon(t)$	Additional reward term in RL based on derivatives and redundancy
ω_h	The weight of first derivative in the additional reward term $\epsilon(t)$
$\omega_{\Delta h}$	The weight of second derivative in the additional reward term $\epsilon(t)$
$\alpha_i(t)$	Binary variable determining the term to be reward/penalty
$h_i(t)$	The first derivative of traffic state at time t
$\Delta h_i(t)$	The second derivative of traffic state at time t

$$n_{ij}(t) \geq 0 \tag{7}$$

$$n_i(t) \leq n_{i,\text{cap}} \tag{8}$$

$$u_{\min} \leq u_{ij}(t) \leq u_{\max} \tag{9}$$

Intraregional and interregional vehicle accumulation, i.e., $n_{ii}(t)$ and $n_{ij}(t)$ are non-negative values, and $n_{i,\text{cap}}$ is the maximal possible number of vehicles accumulated in the region i. At this vehicle accumulation, a gridlock will occur in the network. $u_{\min}$ and $u_{\max}$ represent the lower and upper limit for the perimeter control variable $u_{ij}(t)$ for both directions and such applications are in line with Geroliminis et al. (2013); Zhou and Gayah (2021). These bounds are due to the fact that perimeter control is normally implemented through signalization. While $u_{\max}$ accounts for the lost time caused by the interchange between the red and green phases, $u_{\min}$ is necessitated since an indefinite long red light is rare in real-world cases.

In contrast to the control-based strategies, for the RL-based algorithms, following the idea of redundancy, an additional term $\epsilon(t)$ is added into the objective function J_{RL}, referred to as reward $r_t \in \mathcal{R}$ in the context of RL, leading to:

$$J_{\text{RL}} = \max_{u_{ij}(t)} \int_0^{t_{\text{end}}} [\sum_{i=1,2} M_{ii}(t) + \epsilon(t)]dt \tag{10}$$

The term $\epsilon(t)$ aims to build up a proper redundancy so that the proposed RL algorithm does not reward the agent for targeting the exact critical accumulation point. A comprehensive explanation of the term $\epsilon(t)$ for the reward in RL will be provided in the following Section 4.3.

4. Methodology

This section gives a brief explanation of how MPC and RL are applied in this paper, and how we design an antifragility perimeter control strategy based on the derivatives and redundancy in detail.

4.1. MPC with average history disruption

MPC is an established control method with wide applications in engineering to regulate dynamic systems (Qin and Badgwell, 2003), and is used as one of the benchmark methods in this work. First applied in Geroliminis et al. (2013), MPC has been proven to be an effective and robust method to regulate perimeter control in comparison to a greedy controller. For details of the implementation of MPC in general practice or under the context of perimeter control, we refer the readers to Darby and Nikolaou (2012) and Geroliminis et al. (2013). The applied MPC toolkit in this paper is introduced in Lucia et al. (2017), which uses the CasADi framework (Andersson et al., 2019) and the NLP solver IPOPT (Wächter and Biegler, 2006).

The drawback associated with MPC lies in its presumption of ample a priori knowledge, which includes traffic demand at each time step. However, such data is rarely accessible in practical real-world scenarios. Although traffic forecasting Vlahogianni et al. (2014) may serve as a substitute for traffic demand, the prediction accuracy is not always guaranteed with all sorts of disruptions in the real world. To make the MPC less sensitive to disruptions, in our study, the benchmark MPC algorithm averages all the historical profiles, including both normal and disruption profiles, and uses this aggregated profile as part of the simulation environment.

4.2. RL algorithm

In RL algorithms, an agent or multiple agents interact with a preset environment and improve the performance of decision-making, defined as action a_t in an action space $\mathcal{A}$, based on the observable state s_t in the state space $\mathcal{S}$ and the reward, defined as $r_t = \mathcal{R}(s_t, a_t)$, where $\mathcal{R}$ is the reward function. The improvement of decision-making is commonly realized through a deep neural network as a function approximator. The RL algorithm applied in this work is Deep Deterministic Policy Gradient (DDPG) as proposed in Lillicrap et al. (2015). By applying an actor-critic scheme, DDPG can manage a continuous action space instead of only choosing from a limited set of discrete values as in the Deep Q-Network (DQN) algorithm (Mnih et al., 2013), which are commonly applied as Table 1 shows. Also, Zhou and Gayah (2021) has demonstrated that an RL algorithm with continuous action space can achieve better performance compared to discrete action space. The DDPG algorithm can be divided into two main components, namely the actor and the critic, which are updated at each step through policy gradient and Q-value, respectively. The scheme of the DDPG algorithm applied in this paper is schematically illustrated in Figure 2.

The state $s_t \in \mathcal{S}$ is defined distinctively according to different methods applied in this work. Our proposed method consists of three terms, the vehicle accumulation regarding the OD pair $n_{ij}(t)$, the change rate of vehicle accumulation at each time step $dn_{ij}(t)$ (first derivative) as well as the second derivative $d^2n_{ij,t}$. In Zhou and Gayah (2021), a state s_t defined as $[n_{ij}(t), q_{ij}(t)]$ is adopted. However, since traffic demand in the real world is hardly measurable, $q_{ij}(t)$ would be an unobservable state for the agent. The action $a_t \in \mathcal{A}$ is defined the same as the control variables $u_{ij}(t)$. For the reward r_t, while Zhou and Gayah (2021) uses merely the completion rate, in our proposed method, the reward is defined with an additional $\epsilon(t)$ term, as Eq. 10 shows.

The actor-network is represented by $\mu(\cdot)$ and it determines the best action a_t, which is the percentage of vehicles that are allowed to travel across the periphery, based on the current state s_t and the weight parameters at a certain time step t:

The nature of the best action a_t was also explored in the previous work of Axenie (2022), where in the framework of variable structure control, the authors demonstrate the need for a discontinuous signal. The critic network, denoted by $Q(\cdot)$, takes the responsibility to evaluate whether a specific state-action pair at a certain time step yields the maximal possible discounted future reward $Q(s_t, a_t)$. A common technique used in DDPG is to create a target actor network $\mu'(\cdot)$ and a target critic network $Q'(\cdot)$, which are a copy of the original actor and critic network but updated posteriorly to stabilize the training process and prevent overfitting (Zhang et al., 2021). The target maximal discounted future reward for the target critic network can be calculated as in Eq. 11.

$$y_i = r_i + \gamma Q'(s_{i+1}, \mu'(s_{i+1}|\theta^{\mu'})|\theta^{Q'}) \tag{11}$$

Similar to DQN, the critic network can be updated by calculating the temporal difference between the predicted reward and the target reward and minimizing the loss for a mini-batch N sampled from the replay buffer:

$$L = \frac{1}{N}\sum_i (y_i - Q(s_i, a_i|\theta^Q))^2 \tag{12}$$

Afterward, the actor network can be updated with sampled deterministic policy gradient (Silver et al., 2014):

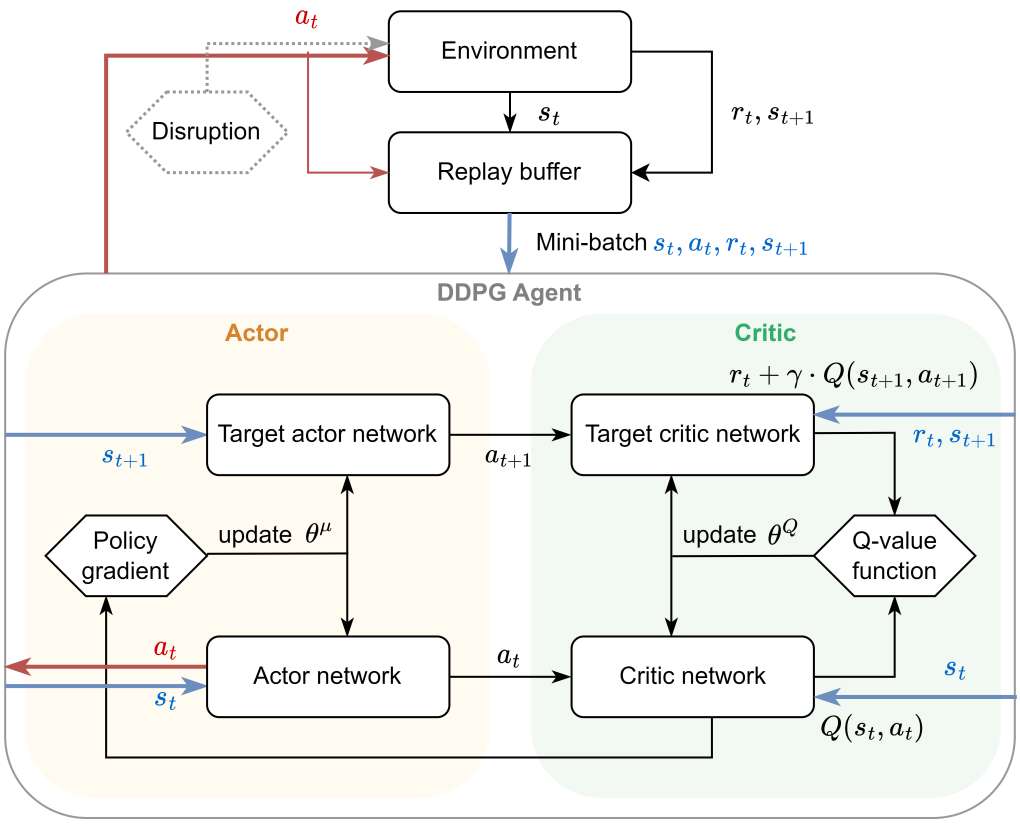

Figure 2: DDPG scheme

$$I = \mathbb{E}_{s_t \sim \rho^\beta}[r(s, \mu(s|\theta^\mu))|_{s=s_t}] \tag{13}$$

$$\nabla_{\theta^\mu} I = \mathbb{E}_{s_t \sim \rho^\beta}[\nabla_a Q(s, a|\theta^Q)|_{s=s_t, a=\mu(s_t)} \nabla_{\theta_\mu} \mu(s|\theta^\mu)|_{s=s_t}] \tag{14}$$

$$\nabla_{\theta^\mu} I \approx \frac{1}{N} \sum_t \nabla_a Q(s, a|\theta^Q)|_{s=s_t, a=\mu(s_t)} \nabla_{\theta^\mu} \mu(s|\theta^\mu)|_{s_t} \tag{15}$$

When training the agent, we add disruptions into the simulation environment starting from a certain training episode, in the form of surging traffic demand or MFD disruption. These various forms of volatility ought to optimally elicit various learning and decision-making processes. The RL agent would include the results of their prior choices to create and update their weight parameters in a situation with high outcome volatility, and being capable of generating and updating expectations after sensing a change in a high-volatility environment.

4.3. Antifragility and the antifragile terms in RL

In our work, following the same idea of modifying the state space $\mathcal{S}$ as in the research works in Tabel 1, we add additional terms based on derivatives (Taleb and Douady, 2013) and redundancy (de Bruijn et al., 2020), in both the state space $\mathcal{S}$ and the reward function $\mathcal{R}$ of the RL algorithm.

For the state space $\mathcal{S}$, we replace q_{ij} using the first and second derivatives of the vehicle accumulation $dn_{ij}(t)$ and $d^2n_{ij}(t)$. With this additional information, the RL agent is aware of a possible demand surge of MFD disruption and $d^2n_{ij}(t)$ can reflect the curvature of such changes.

For the reward function $\mathcal{R}$, the trip completion at each time step acts as the main component of our proposed method. The term $\epsilon(t)$ in the objective function J_{RL} in Equation (10) acts as an additional term to build up redundancy in the system. Similar to the creation of the additional term in the state space, we create redundancy also through the calculation of the derivates, but instead of the derivatives of the vehicle accumulation, we calculate the derivatives of the traffic state. This creates a one-to-one correspondence between the derivatives of the vehicle accumulation and the derivatives of the traffic state. To explain this antifragile term in the reward, we summarize $\epsilon(t)$ as the sum of two terms, with $H(t)$ being an overall term representing the first derivative of the traffic state and $\Delta H(t)$ representing the second derivative:

$$\epsilon(t) = H(t) + \Delta H(t) \tag{16}$$

Here, $H(t)$ and $\Delta H(t)$ can be expanded as:

$$H(t) = \sum_{i=1,2} H_i(t) = \omega_h \sum_{i=1,2} f(n_i(t), n_{i,\mathrm{crit}}, n_{i,\mathrm{cap}}) \cdot \alpha_i(t) \cdot h_i(t) \tag{17}$$

$$\Delta H(t) = \sum_{i=1,2} \Delta H_i(t) = \omega_{\Delta h} \sum_{i=1,2} f(n_i(t), n_{i,\mathrm{crit}}, n_{i,\mathrm{cap}}) \cdot \Delta h_i(t) \tag{18}$$

$h_i(t)$ and $\Delta h_i(t)$ are the first and second numerical derivatives of the traffic states on the MFD, $h_i(t)$ is defined as the difference of trip completion over vehicle accumulation at the end of a time step versus at the beginning of the same time step, as in Eq. 19 shows, and the second derivative $\Delta h_i(t)$ is calculated as the difference between the first derivatives of two consecutive time steps, as in Eq. 20 shows:

$$h_i(t) = \frac{M_i(t) \ - \ M_i(t-1)}{n_i(t) \ - \ n_i(t-1)} \tag{19}$$

$$\Delta h_i\,(t) = h_i\,(t) - h_i\,(t-1) \tag{20}$$

Since in the RL algorithms implemented in this paper, all variables involved in the deep neural network should be normalized to facilitate the training process, meaning the exact values of the derivatives are not of importance, ω_h and $\omega_{\Delta h}$ are introduced as the weight constants for the first and second derivatives to regulate their impact on the reward side $\mathcal{R}$.

The binary variable $\alpha_i(t)$ was designed in the first derivative to reward the agent when moving towards the desired direction on the MFD. For instance, the derivative of any data point in the congested zone of the MFD is negative. In this case, when the vehicle accumulation is still getting larger, a penalty will be applied. However, if the vehicle accumulation is decreasing through perimeter control, this binary $\alpha_i(t)$ variable will turn it into a reward. For the second derivative, an additional binary variable is not necessary since the two consecutive first derivatives are able to determine whether $\Delta h_i(t)$ is either positive or negative.

$$\alpha_i(t) = \begin{cases} 1, & \text{if } n_i(t) \geq n_i(t-1), \\ -1, & \text{otherwise.} \end{cases} \tag{21}$$

The term $f(n_i(t), n_{i,\mathrm{crit}}, n_{i,\mathrm{cap}})$ is a reduction factor to constrain the impact of the $\epsilon(t)$ term when the accumulation is either on a very lower level (empty network) or on a very higher level (gridlock). The area near the critical accumulation is where the $\epsilon(t)$ term should have the

greatest impact. Here we use a modified trigonometric function to realize this purpose. It should be noted that other functions, such as normal distribution, are also valid for achieving the same purpose.

$$f(n_i(t), n_{i,\text{crit}}, n_{i,\text{cap}}) = \begin{cases} \dfrac{1 + \cos\Big(-\pi \cdot \dfrac{n_{i,\text{crit}} - n_i(t)}{n_{i,\text{crit}}}\Big)}{2}, & \text{if } n_i(t) \geq n_{i,\text{crit}}, \\ \dfrac{1 + \cos\Big(-\pi \cdot \dfrac{n_i(t) - n_{i,\text{crit}}}{n_{i,\text{cap}} - n_{i,\text{crit}}}\Big)}{2}, & \text{otherwise.} \end{cases} \tag{22}$$

After considering all the modifiers above, we show $H(t)$ and $\Delta H(t)$ using a single MFD as an example in Figure 3 and 4. The first derivative $H(t)$, in Figure 3(a), rewards the agent more when it's moving towards the critical accumulation to maximize its trip completion rate. However, when the number of vehicles approaches the critical accumulation, this term drops significantly and becomes a penalty when it exceeds the critical point. Since the first derivative $H(t)$ is a complementary term in addition to the trip completion in the reward function, we showcase the influence of this term on the MFD after normalization in Figure 3. With increasing weight coefficient ω_h, the critical accumulation of the modified MFD becomes marginally smaller compared to the original MFD, and the reward that the RL agent can receive also decreases faster after the accumulation exceeds the critical accumulation. Although the trip completion still follows the original MFD in the simulation environment, The agent learns to get more rewards following the modified MFD. In this way, redundant overcompensation has been established to prevent accumulation from exceeding the critical accumulation when disruption takes place unexpectedly.

An interesting note is that estimation uncertainty, also known as second-order uncertainty, is another factor that affects disruptions that take place unexpectedly. This is in fact the imprecision of the learner's current beliefs about the environment, and what the antifragile terms capture. This amount reduces with sampling if beliefs are acquired by learning as opposed to instruction (e.g. anticipation through redundant overcompensation). When estimating uncertainty is substantial, unlikely samples could partly be attributed to the agent's false assumptions about the environment's structure rather than a change in that structure (e.g. around critical accumulation).

The second derivative $\Delta H(t)$ is shown in Figure 4. The x-axis is the vehicle accumulation, same as in Figure 3(a), while the y-axis represents how fast the traffic state is changing on the MFD. The faster it increases to reach the critical accumulation, the greater the penalty will be applied to the RL agent. This observation is consistent with the redundant overcompensation and time-scale separation principles formalized in Taleb and Douady (2013) and practically applied in Axenie (2022) and Axenie and Saveriano (2023). On the contrary, if the vehicle accumulation decelerates, a reward will be applied. Similar to $H(t)$, this complementary term $\Delta H(t)$ is also dependent on the normalization factor $\omega_{\Delta h}$.

With $H(t)$ and $\Delta H(t)$, the agent learns to be conservative when regulating the perimeter control variables when the accumulation is about to reach critical, in case disruptions take place. Therefore, as can be concluded, although $H(t)$ and $\Delta H(t)$ apply the same concept of the derivative as the $dn_{ij}(t)$ and d^2n_{ij} in the state space $\mathcal{S}$, the purpose of $H(t)$ and $\Delta H(t)$ is preserving redundancy in the system instead of feeding additional information to the agent. This behavior is consistent with the locally discontinuous shape of the action signals $u_{ij}(t)$ applied to

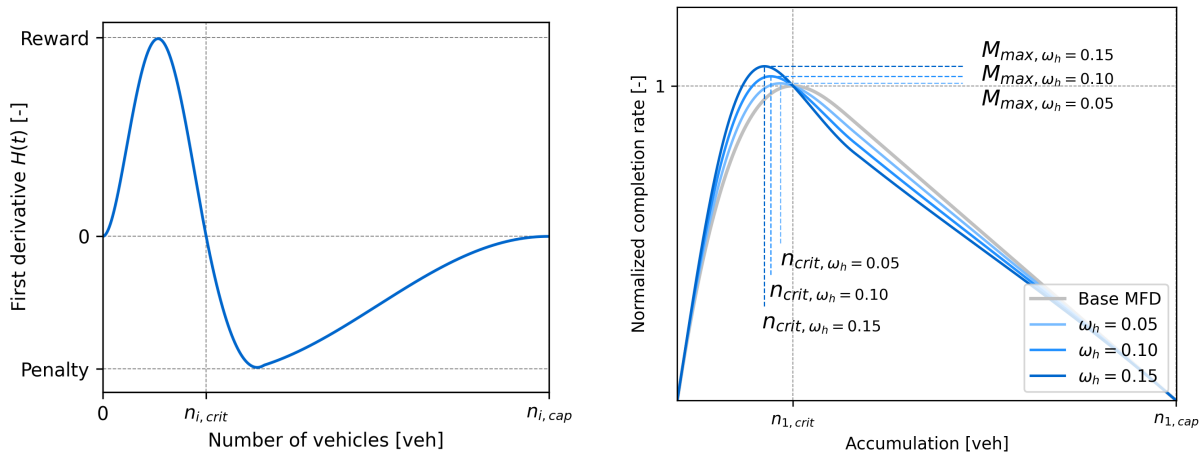

(a) H for the first derivative $h_i(t)$.

(b) ΔH for the second derivative $\Delta h_i(t)$.

Figure 3: Illustration of the term $H(t)$ and its effect on the MFD

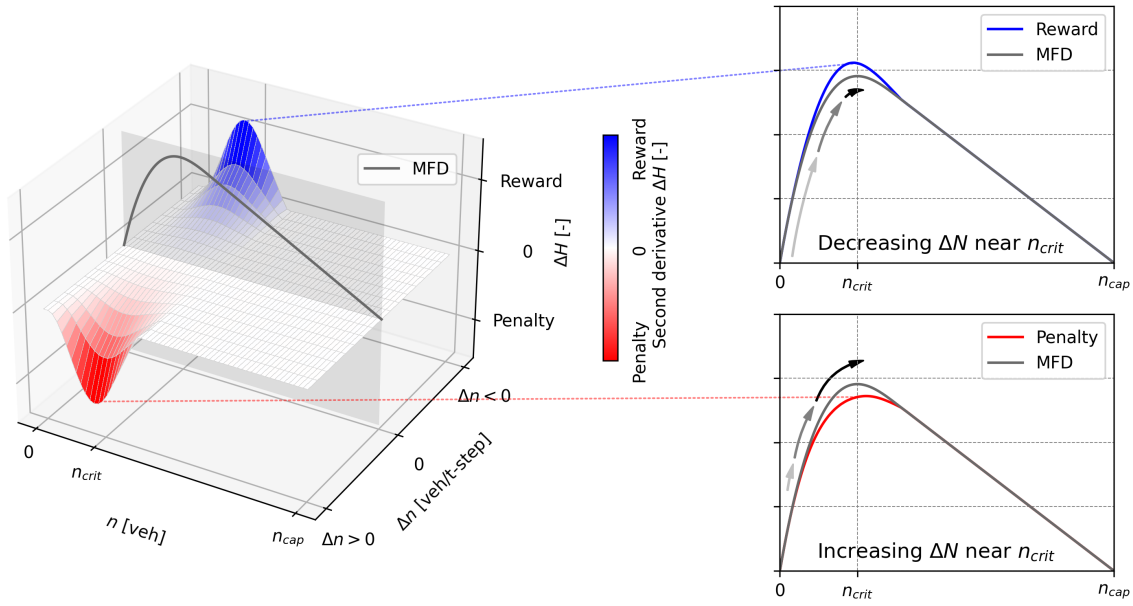

Figure 4: Illustration of the term $\Delta H(t)$

the cordon network, as suggested by the control theoretic study of Axenie (2022).

5. Experiment application

This section introduces the environment setup of the simulation and the evaluation procedure. We investigate a total number of three perimeter control strategies in addition to a no-control scenario, based on 2 different scenarios, i.e., under constant or incremental disruptions for testing proto-antifragility and progressive antifragility respectively:

- No control

- MPC modified from (Geroliminis et al., 2013), averaging all history profiles including disruption as a new demand or MFD profile.

- State-of-the-art RL-based method proposed by (Zhou and Gayah, 2021) as baseline:
  State s_t: vehicle accumulation and traffic demand $[n_{ij}(t), q_{ij}(t)]$
  Reward r_t: trip completion in both regions $[\sum_{i=1,2} M_{ii}(t)]$

- The proposed RL-based antifragile method:
  State s_t: vehicle accumulation and its derivatives $[n_{ij}(t), dn_{ij}(t), d^2n_{ij}(t)]$
  Reward r_t: trip completion and the $\epsilon(t)$ redundancy term $[\sum_{i=1,2} M_{ii}(t) + \epsilon(t)]$

5.1. Simulation environment parametrization

As introduced in Section 3, we simulate a cordon-shaped urban network with inner and outer regions with different MFDs. Some minor modifications have been adapted in the congested zone of the MFD to ensure the derivative of the MFD is continuous. The MFD of the outer region is largely in line with the observations in Yokohama (Geroliminis and Daganzo, 2008). Other critical indicators, e.g., critical accumulation and maximal trip completion, remain unchanged. The non-identical MFDs reflect the fact that the area of the periphery is much larger than the city center, and thus the maximal accumulation would be significantly higher. The traffic demand under no disruption is approximated based on Geroliminis and Daganzo (2008). Instead of a trapezoidal demand profile, the chosen profile is in the shape of a normal distribution in accordance with Mazloumi et al. (2010) to describe the peak hour traffic flow. The total simulation duration t_{end} is 2 hours with each time step Δt as 60 seconds, and the second hour has significantly fewer vehicles so that the network would be able to clear the vehicles accumulated in the first hour. Other notable constraints and initializations include the lower and upper bounds for the perimeter control variable $u_{ij} \in [0.1, 0.9]$ (Geroliminis et al., 2013) and an initial accumulation in the network $n_{ij,0} = [600, 1300, 300, 2400]$.

We simulate two different disruption scenarios in our work, namely surging traffic demand and MFD disruption due to adversarial events. Also, as introduced in Section 2, antifragility can be defined in two different levels, i.e., proto-antifragility and progressive antifragility. Therefore, we consider two different disruption profiles regarding each level of antifragility, as shown in Figure 5.

First, to validate proto-antifragility under surging demand, after the agent has been trained for the first 50 episodes with a base demand profile, as shown in Figure 6(a), we introduce a new demand profile with disruption, which characterizes a surging demand within a short period from the outer region into the inner region, as shown in Figure 6(b). The new environment lasts for another 50 episodes with a constant magnitude of 2,500 vehicles following normal distribution. On the other side, to test progressive antifragility, instead of a constant magnitude of disruption, an incremental disruption is applied for another 50 episodes following the training with 50 episodes of the based demand profile. The magnitude of disruption grows linearly from 0 to 5,000 vehicles, which is twice the number of vehicles in the constant disruption. Both the RL-based methods are trained 15 times and the average is calculated as their learning curves.

Some adversarial events will exert a negative effect on the MFD, leading to a worse roadside performance. However, since these events may take place in different forms, weather, accidents, blockage, etc., little research effort has been made to unveil the exact correlation between each type of event and the change of the MFD. Hence, we simulate three possible MFD disruption profiles and assume these profiles can account for the majority of the possible negative consequences.

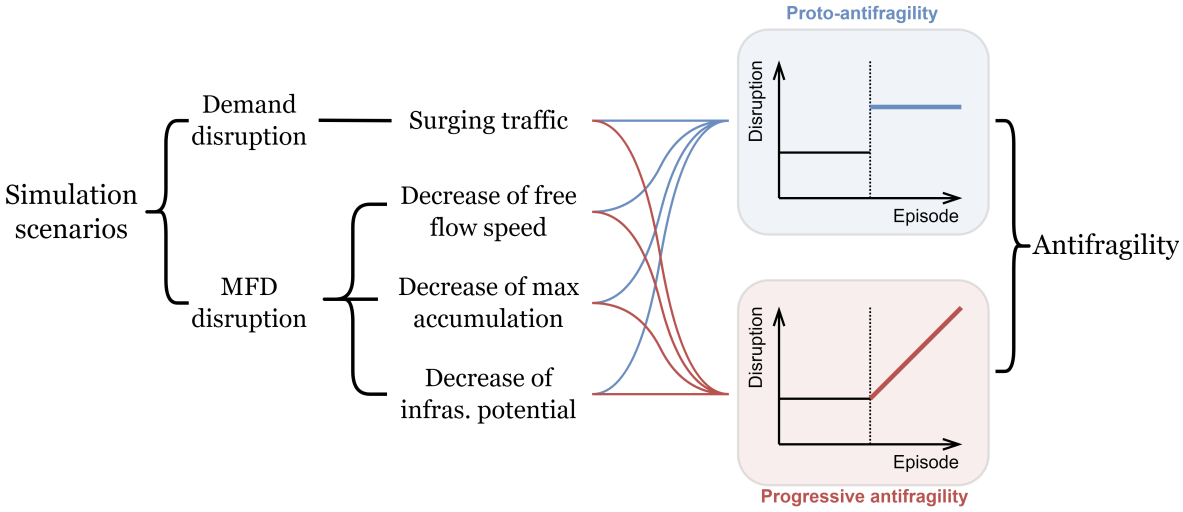

Figure 5: Illustration of simulation scenarios

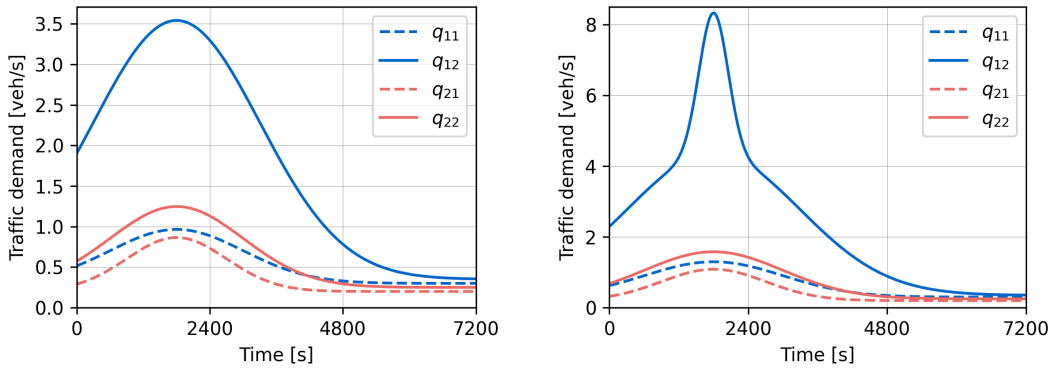

(a) Base demand profile

(b) Demand profile under disruption

Figure 6: Demand profile with or without surging demand

The first profile is a decrease of the free flow speed without critical and maximal accumulation dropping, as shown in Figure 7(a) representing the MFD of the inner region. This can be caused by unfavorable weather, such as slippery and icy roads or low visibility. The second profile, Figure 7(b), is a decrease of critical density without a reduction of the free flow speed. For example, road maintenance work on an arterial road can significantly reduce the serviceability of this region. The last profile is based on Ambühl et al. (2020), in which a parameter λ is defined as the infrastructure potential to quantify the decrease of flow values due to infrastructure, between-vehicle interactions, etc. Networks in the real world can have a λ around $0.03 - 0.07$ and a greater λ indicates the infrastructure is less efficiently utilized. Since this method is based on the method of cuts (Daganzo and Geroliminis, 2008) instead of a polynomial function, the shape of the MFD for this profile is marginally different from the other two MFDs.

For the first two profiles, while proto-antifragility is validated with a 12.5% drop of the maximal flow, progressive antifragility is tested against an increasing value of drop from 0% to 25%. For the third MFD profile, a constant λ of 0.095 is applied to test the proto-antifragility, and the λ increases from 0.07 to 0.12 to represent the growing magnitude of disruption as the simulation environment for exhibiting progressive antifragility. Interestingly, these three profiles

also represent three different patterns of how the critical accumulation evolves with the drop of flow values, i.e., constant, decreasing, and increasing critical vehicle accumulation.

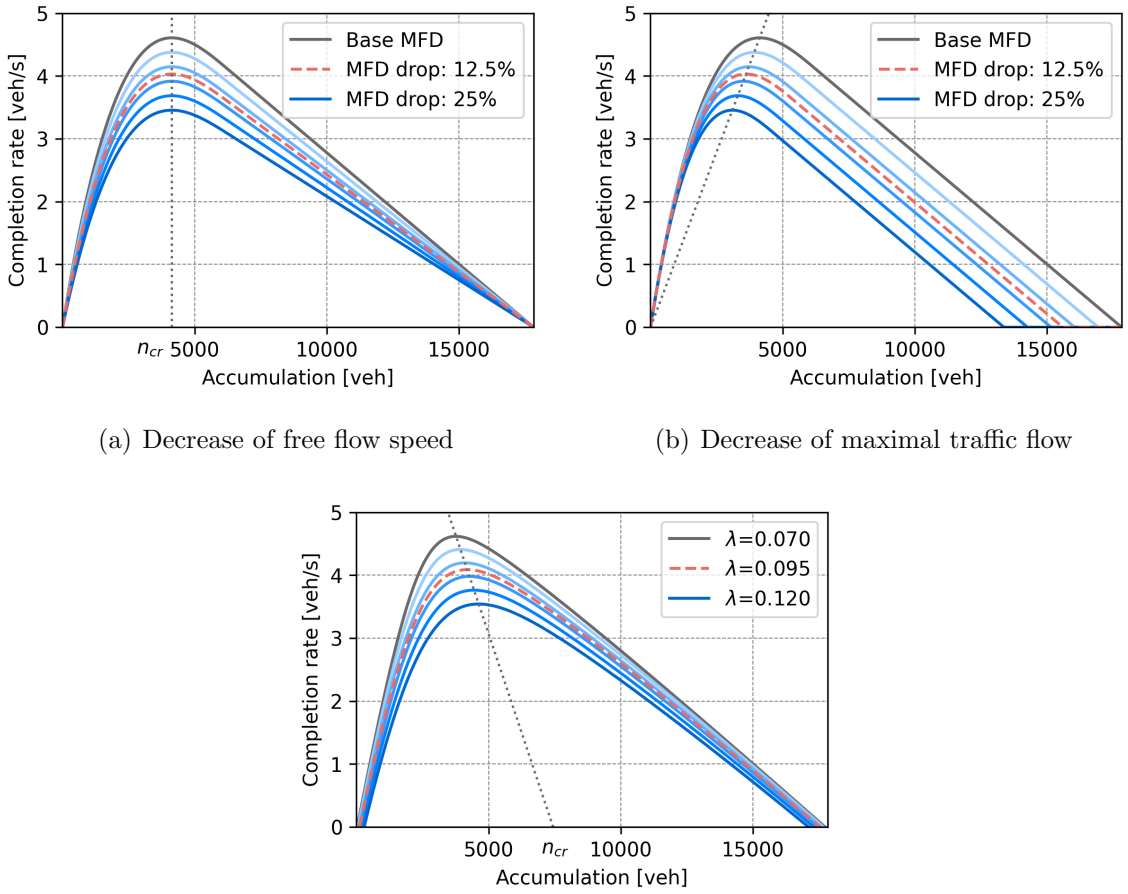

(a) Decrease of free flow speed

(b) Decrease of maximal traffic flow

(c) Decrease of infrastructure potential

Figure 7: MFD change due to adversarial events

5.2. Performance evaluation

Although the reward defined in the RL algorithm is based on trip completion, to better showcase antifragility, the main performance indicator being evaluated here is the Total Time Spent (TTS), which is calculated by adding up the number of vehicles within the network at each second of the simulation. The main reason for choosing TTS over completion is that completion is lower bounded with increasing magnitude of disruption by the number of vehicles that finished their trips before the disruption, meaning we may observe a concave trip completion with increasing disruptions at first but then it becomes approximately constant. This makes the manifestation of antifragility difficult since the performance curve could be partially concave and partially convex. However, by using TTS as the performance indicator, we circumvent this problem since TTS still grows linearly with increasing disruptions even under extreme cases instead of being lower-bounded. Therefore, the full convexity or concavity of the performance curve can be maintained and we can roughly approximate the simulation results with a second-degree polynomial.

As urban road networks are always subject to capacity constraints, fully antifragile traffic control strategies may be impossible to design. Therefore, we normalize all the other perimeter control strategies over the RL baseline method to study the relative antifragility. To quantify the progressive antifragility of different methods, we calculate the skewness of the TTS distribution. A negative value of skewness indicates the distribution has a longer or fatter left tail and thus a higher degree of concavity in the function.

6. Results

This section presents the simulation results of the four methods, i.e., no-control, MPC, baseline RL-based method, and our proposed antifragile RL-based method under the two scenarios to show the property of proto-antifragility and progressive antifragility, respectively.

6.1. Proto-antifragility

Systems with the property of proto-antifragility can learn from past adverse events and anticipate possible ongoing disruptions of similar magnitudes to enhance future performance. To validate this property, we apply disruptions with constant magnitude after training the agent with the base demand profile for a certain number of episodes.

6.1.1. Surging traffic demand

Unlike the no-control and MPC approaches, RL-based methods are subject to performance variations over simulation episodes. Therefore, in Figure 8, besides the performance curves of the no-control and MPC approaches, we also show the learning curves of the baseline RL method and our proposed antifragile RL method. The curves are averaged from 15 simulations, while the shadowed area indicates the standard deviation of the simulation results. After conducting 50 episodes of training together with testing under disruptions, the performance of different algorithms under no disruptions is then again validated. Hence, an addition of 2 testing phases was implemented under and under no disruption, using the weight parameters of the neural networks obtained from the last training episode.

It can be noticed that two significant phenomena occurred during the initial 50 episodes with the base demand. First, the proposed antifragile method can achieve better performance with less TTS when there is no disruption in the network. While the baseline method has almost converged after 50 episodes, the proposed antifragile method seems to be capable of further improving the performance with more training episodes. The reason for not continuing the training process until the convergence of both methods is to avoid overtraining the non-disruption-related weight parameters as well as the underfitting of the disruption-related parameters. In addition, the shadowed area of our proposed method represents a less significant performance variation of about 6.0% less compared to the baseline method, based on the averaged performance between episodes 30 and 50. This indicates that the proposed antifragile method exhibits comparably higher training stability.

After disruption with constant magnitude is introduced into the network. The performance of the two RL-based methods has first changed drastically. Then, while the proposed method has an obvious tendency to reduce TTS over the following 50 episodes, the baseline method shows little sign of improving performance. Also, the training stability of the proposed method becomes increasingly stable over episodes as the width of the shadowed area gets smaller.

While the results of testing under disruption follow the same pattern as the last episode of the training process, however, when the simulation environment reverts to the previous no-disruption

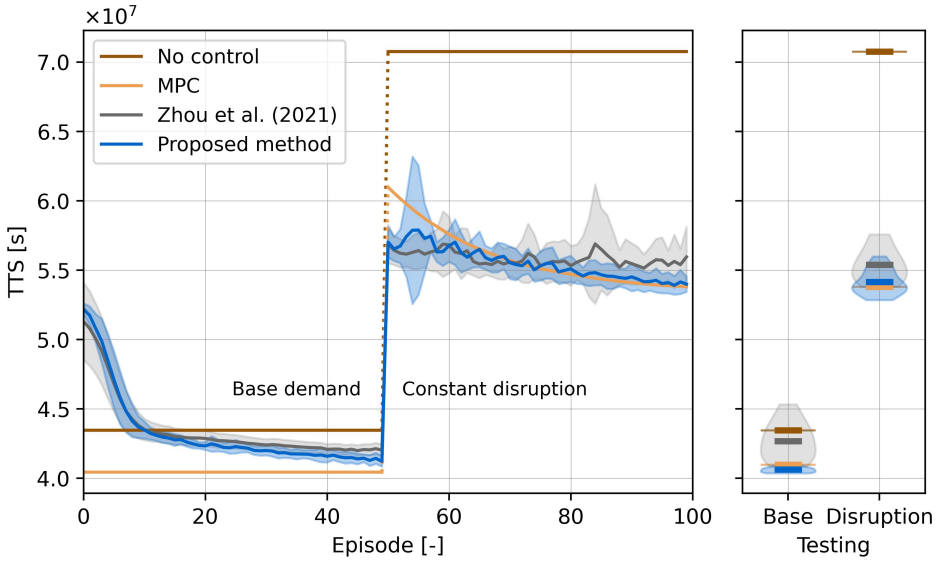

Figure 8: Performance curves under constant disruptions

condition, the performance of different methods behaves differently. Since our modified MPC averages demand history, after experiencing episodes with disruptions, performance deterioration of 1.3% can be observed when there is no disruption. A similar pattern can be observed for the baseline RL method. Not only is the TTS 1.5% higher in this testing episode compared to the training episode 50, but the performance variation is also significantly larger. On the contrary, our proposed antifragile RL method can both maintain excellent performance and achieve smaller variation.

We normalize all the other methods over the result of the baseline RL-based method averaged from the 15 simulations, as shown in Figure 9. The performance improvement of both MPC and the proposed antifragile methods can be observed. Since we average all the past experiences of the demand profile, including disruptions for MPC, it is capable of performing better under the same disrupted scenario, and even marginally better than the proposed antifragile method. Therefore, MPC can, to some extent, demonstrate the property of proto-antifragility. While maintaining roughly similar performance compared to the baseline method at the beginning of the scenario switch, and thus better performance than MPC, the proposed method gains capability in dealing with disruptions when experiencing more and more disruptions of the same magnitude, and reaches a reduction of 4.9% of TTS in the final episode compared to the baseline RL method. This also demonstrates the property of proto-antifragility.

6.1.2. MFD disruption

Here we showcase the performance of different methods under the influence of three MFD disruption scenarios, as illustrated in Figure 5, namely decrease of free flow speed, decrease of max accumulation, and decrease of infrastructure potential, and these three scenarios correspond to the MFD profiles in Figure 7. After 50 episodes of training without disruption, we introduce a constant magnitude of disruption into the simulation environment, in the form of an MFD capacity drop, for another 50 episodes. Figure 10 shows the simulation results of the three MFD disruptions. The comparison between these three MFD disruption settings first shows that, for the baseline RL method, the difficulty in adjusting to new MFD profiles is different. While Figure

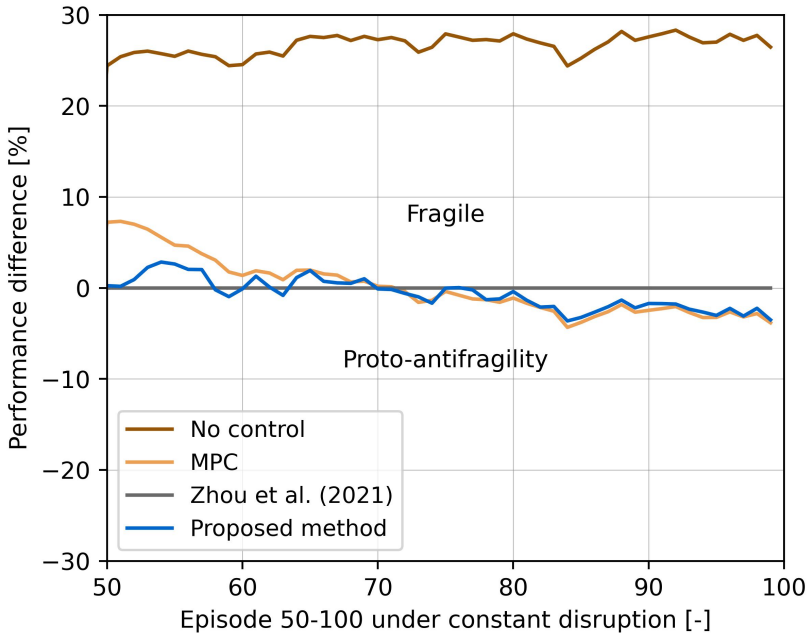

Figure 9: Performance difference normalized over the baseline method under constant disruptions

10(b) with decreasing maximal traffic flow demonstrates that the baseline RL method gradually adapts to the new profile, Figure 10(c) shows little sign of the baseline method learning from disruptions. Figure 10(a) exhibits the adaptation to a certain degree between the other disruption profiles. It is speculated that since the shape of MFD remains unchanged in Figure 10(b), this creates a less deviated scenario for the RL agent to learn, whereas the change of the MFD profile is the greatest in Figure 10(c) as the critical accumulation also increases during such disruptions. That being said, the learning curves from the proposed antifragile method demonstrate noticeable performance improvement in all three MFD disruption scenarios, indicating its property of proto-antifragility. Also, the standard deviation indicated by the shadowed area of the proposed antifragile method is also significantly smaller compared to the baseline method in Figure 10(a) and 10(c).

6.2. Progressive antifragility

Progressive antifragility describes a system that exhibits a nonlinear response to a linearly increasing magnitude of volatility. In terms of TTS, since an increase in the traffic density or vehicle accumulation within the network will result in a decrease in the vehicle speed or trip completion rate, and inevitably increase the TTS, a concave response between TTS and vehicle accumulation can indicate a progressive antifragile system.

6.2.1. Surging traffic demand

The four studied methods are tested in an environment with linearly increasing traffic demand for 50 episodes after being trained with the same base demand as in the previous scenario for 50 episodes. Furthermore, another testing phase of 20 episodes is carried out following the same demand increment and the demand magnitude of the last training episode. Figure 11 shows the TTS of different methods under incremental disruptions in both training and testing phases. It

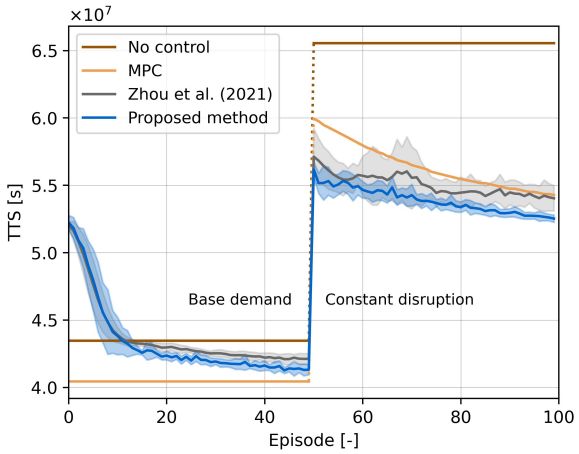

(a) Decrease of free flow speed

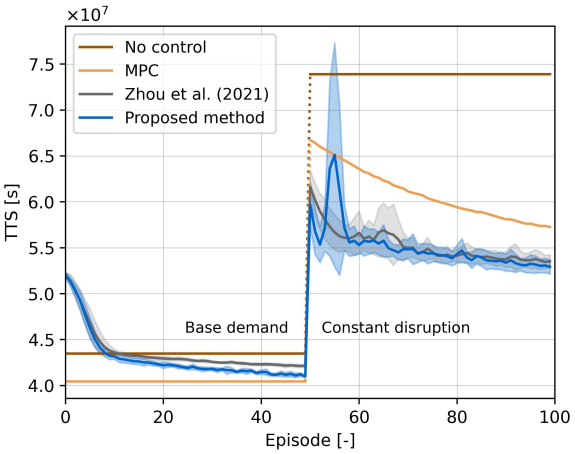

(b) Decrease of maximal traffic flow

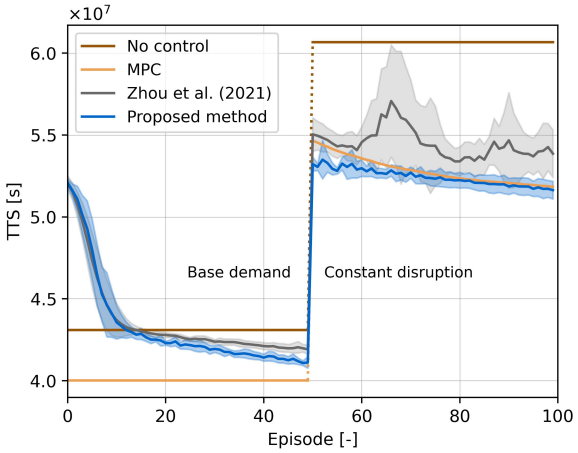

(c) Decrease of infrastructure potential

Figure 10: MFD change due to adversarial events

should be noted that Figure 11(a) and Figure 11(b) do not share the same y-axis and the result of the no-control approach is not presented in 11(b) due to its exceedingly high value.

Under this scenario, the TTS of the no-control approach grows sharply, doubling the difference between the last and the first episode under the incremental disruption of the other methods. The performance deviation of the proposed method is relatively low compared to the baseline method under the disruptions scenario. However, the performance deviation of both methods grows with the increase in the magnitude of disruption. The deviation of the baseline method is significantly larger compared to the proposed antifragile method in the last simulation episodes. Although the performance of MPC under the constant disruptions scenario is marginally better than the proposed antifragile method, the performance falls behind the other 2 RL-based methods, as the magnitude of the disruption remains low and grows linearly after the first 50 episodes. Therefore, when averaging the past demand experiences with increasing disruptions, MPC cannot gain sufficient knowledge of the upcoming magnitude of the disruptions. In the testing phase, it can be observed that the performance deviation of the baseline RL method is significantly larger

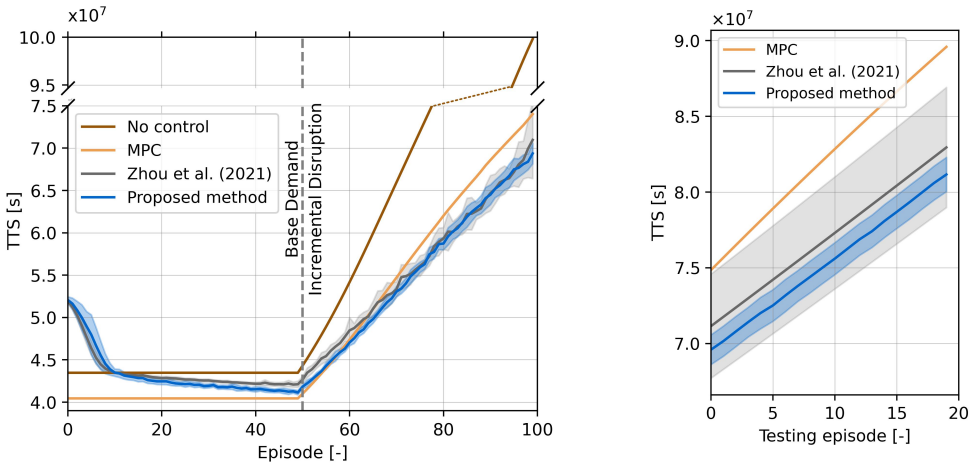

(a) Training for 50 episodes

(b) Testing for 20 episodes

Figure 11: Performance curves under incremental disruptions

compared to the proposed antifragile RL method. Since in the testing phase, the agents' weight parameters are no longer subject to updates as typically observed during the training phase in RL, the performance curves of both RL-based methods appear to be linear.

Since the performance differences between the baseline Zhou and Gayah (2021) and the other methods are hard to observe in this figure, we need to normalize the performance of all the other methods over the baseline methods. Before the normalization process, to better showcase the nonlinear response and compare the concavity or convexity of different methods, the performance deviation in the learning curves of the RL-based methods needs to be minimized. As part of the process, we utilize second-degree polynomials to approximate the performance curves of different methods. After obtaining the polynomial coefficients through fitting, we reconstruct the data points accordingly, with which the normalization process can be implemented, and the results are shown in Figure 12.

One advantage of using a polar coordinate system instead of Cartesian coordinates is its ability to accentuate performance differences, particularly when there is a high level of disruption. While both the no-control approach and MPC exhibit a positive increase in performance compared to the baseline method, the proposed antifragile approach stands out as the only one maintaining a negative difference, with its absolute value becoming even larger once the disruption exceeds approximately 4,000 vehicles. It is important to note that the curvature of the plot in polar coordinates does not necessarily imply that the data points for a specific method follow a concave or convex distribution due to the inherent characteristics of polar coordinates. However, it is evident that the curve representing the proposed method initially approaches the baseline curve, demonstrating, for instance, a performance difference of -0.5% when the disruption shows roughly 3200 additional vehicles. Subsequently, it diverges and reaches -0.5% again with around 5000 vehicles. This behavior indicates that the proposed method exhibits relative concavity when compared to the baseline method, highlighting its progressive antifragility.

Furthermore, for a quantitative comparison of progressive antifragility across various methods, we compute the skewness of each distribution and present the results in Table 3. All three methods exhibit negative skewness values, implying a form of relative progressive antifragility compared to the baseline method. Among them, the no-control approach displays the least

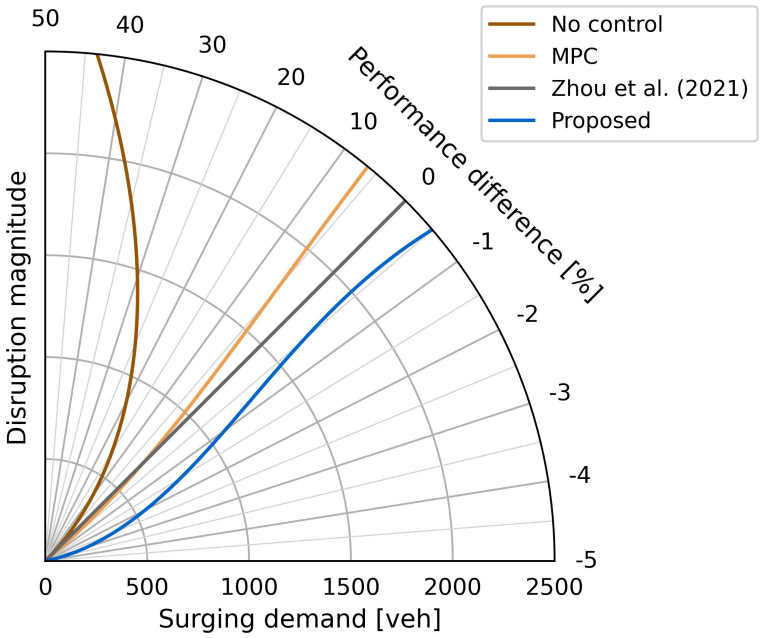

Figure 12: Performance difference normalized over the baseline method under incremental disruptions

degree of relative antifragility, while our proposed antifragile method has demonstrated the most substantial antifragility property, as evidenced by the highest absolute skewness value in its distribution.

Table 3: Normalized skewness over baseline method under incremental traffic demand

Methods	Skewness
No control	-0.326
MPC	-0.753
Antifragile RL-based method	-1.106

6.2.2. MFD disruption

Figure 13 shows the learning curves of the four methods and the performance difference normalized over the baseline method under different MFD disruptions. In general, the performance quantified by TTS shows that our proposed method has a superior performance. More significantly, the skewness of the performance difference curves under all three types of MFD disruptions, as in Table 4 summarized, are negative, showcasing the property of our proposed method being progressively antifragile. In the scenario with the decrease of the critical accumulation, the skewness has reached a value of -0.991, demonstrating the most relative antifragile property of our proposed method compared to the baseline method.

7. Conclusion

This research work introduces the concept of antifragility by comparing it with two other terms robustness and resilience, which are commonly used in transportation and traffic control

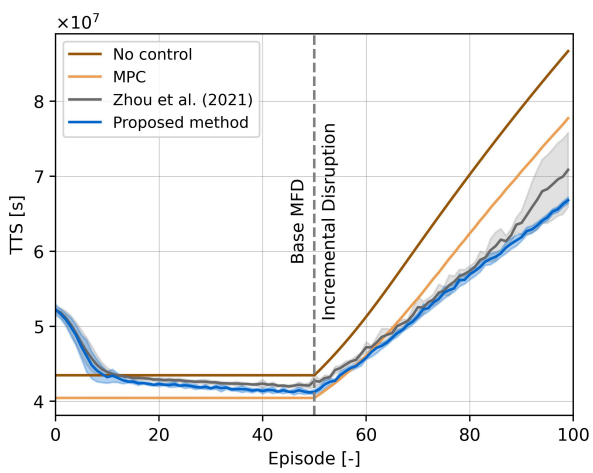

(a) Under decreasing free flow speed

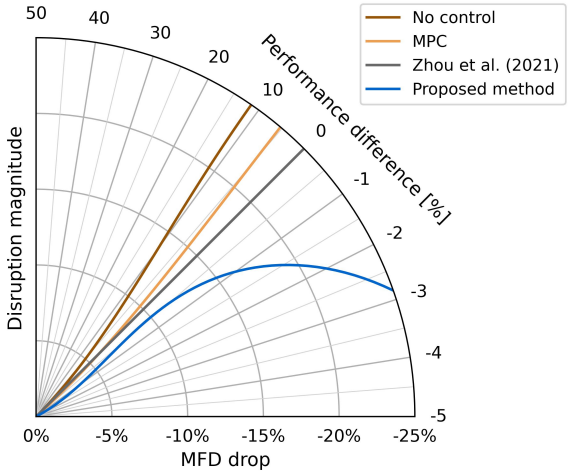

(b) Performance difference

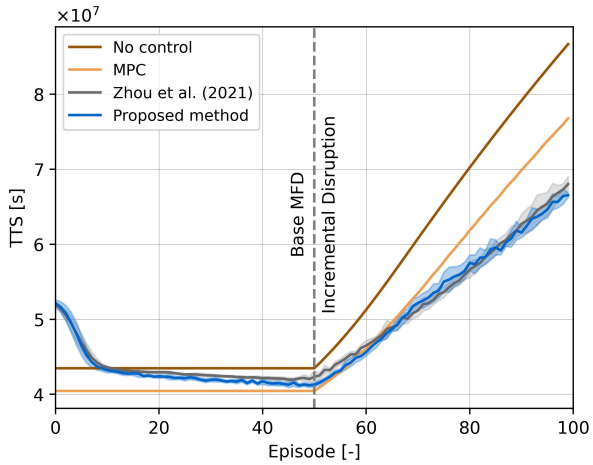

(c) Under decreasing critical flow

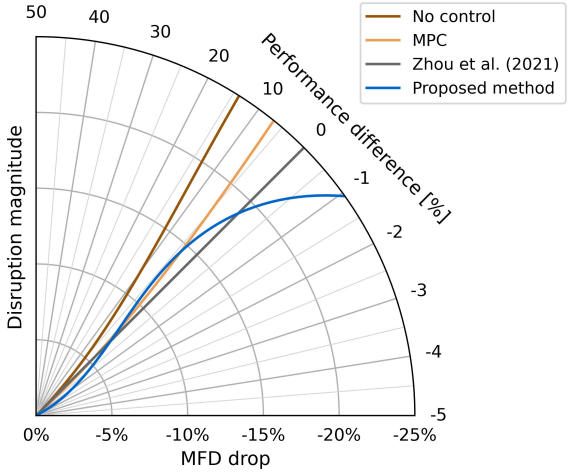

(d) Performance difference

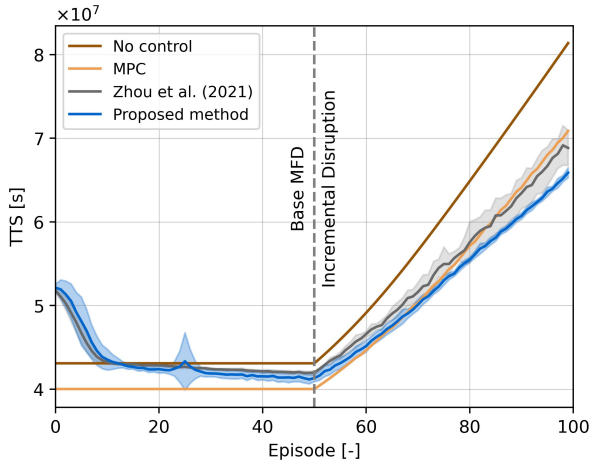

(e) Under infrastructure potential loss

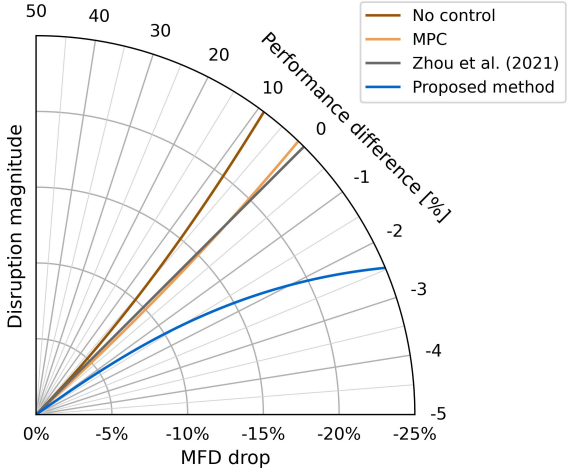

(f) Performance difference

Figure 13: Performance curves under incremental disruptions

Table 4: Normalized skewness over baseline method under growing MFD disruptions

MFD disruption	Skewness
Decrease of the free flow speed	-0.795
Decrease of the critical accumulation	-0.991
Decrease of the infrastructure capacity	-0.392

strategies. Through a literature review on using RL algorithms in traffic control to realize a robust or resilient design, whether and how such properties can be induced in RL is investigated. Following the same idea, we manage to induce antifragility in perimeter control by modifying the state space and reward function based on a state-of-the-art RL-based perimeter control method. We incorporate the change rate and curvature of the traffic states in the state space to leverage the potential of such derivatives to feed more information to the RL algorithm. Also, a redundant overcompensation term in the reward function has been carefully composed to empower the system to be more antifragile to disruptions.

We conducted a comprehensive comparison between our proposed antifragile RL-based perimeter control approach and three other methods: no-control, MPC, and the state-of-the-art RL-based method as a baseline. This comparison was carried out on two different levels, disruptions with constant and incremental magnitude, for validating proto-antifragility and progressive antifragility, respectively. Proto-antifragility describes a system that learns from past experience and increases performance while progressive antifragility depicts a nonlinear response to linearly growing disruption. We investigated two different types of disruptions, namely surging traffic demand and MFD disruptions. The results from the study clearly demonstrated the effectiveness and antifragility of our proposed method, for both proto-antifragility and progressive antifragility. Furthermore, we put forward a novel method for quantification by comparing the skewness of the distribution. Our proposed antifragile method exhibits the greatest negative skewness among the methods examined, indicating its relative progressive antifragility property against disruptions.

In conclusion, this study is the first of its kind to pioneer the application of the antifragility concept in enhancing the daily operation of engineering systems to improve performance during unforeseen disruptions using a learning-based algorithm. It introduces a new possibility for evaluating system operation under disruptive conditions. Moreover, the concept can be extended not only to other traffic control strategies like traffic signal control and pricing but also to various engineering disciplines and industries, broadening its potential impact.

8. CRediT authorship contribution statement

Linghang Sun: Conceptualization, Investigation, Methodology, Visualization, Writing – original draft. Michail A. Makridis: Conceptualization, Methodology, Supervision, Writing - review & editing. Alexander Genser: Methodology, Visualization, Writing - review & editing. Cristian Axenie: Project administration, Resources, Writing - review & editing. Margherita Grossi: Project administration, Resources, Writing - review & editing. Anastasios Kouvelas: Supervision, Writing - review & editing.

9. Declaration of Competing Interest

This research was kindly funded by the Huawei Munich Research Center under the framework of the Antigones project, with one of our co-authors being employed at the said company. Otherwise, the authors declare that they have no known competing financial interests or personal relationships that could have appeared to influence the work reported in this paper.

References

Ambühl, L., Loder, A., Bliemer, M.C.J., Menendez, M., Axhausen, K.W., 2020. A functional form with a physical meaning for the macroscopic fundamental diagram. Transportation Research Part B: Methodological 137, 119–132. doi:10.1016/j.trb.2018.10.013.

Ambühl, L., Loder, A., Leclercq, L., Menendez, M., 2021. Disentangling the city traffic rhythms: A longitudinal analysis of MFD patterns over a year. Transportation Research Part C: Emerging Technologies 126, 103065. doi:10.1016/j.trc.2021.103065.

Ambühl, L., Loder, A., Menendez, M., Axhausen, K.W., 2018. A case study of Zurich's two-layered perimeter control , 8 p.doi:10.3929/ETHZ-B-000206987.

Ambühl, L., Loder, A., Zheng, N., Axhausen, K.W., Menendez, M., 2019. Approximative Network Partitioning for MFDs from Stationary Sensor Data. Transportation Research Record 2673, 94–103. doi:10.1177/0361198119843264.

Andersson, J.A.E., Gillis, J., Horn, G., Rawlings, J.B., Diehl, M., 2019. CasADi – A software framework for nonlinear optimization and optimal control. Mathematical Programming Computation 11, 1–36. doi:10.1007/s12532-018-0139-4.

Aslani, M., Seipel, S., Mesgari, M.S., Wiering, M., 2018. Traffic signal optimization through discrete and continuous reinforcement learning with robustness analysis in downtown Tehran. Advanced Engineering Informatics 38, 639–655. doi:10.1016/j.aei.2018.08.002.

Aven, T., 2015. The Concept of Antifragility and its Implications for the Practice of Risk Analysis. Risk Analysis 35, 476–483. doi:10.1111/risa.12279.

Axenie, C., 2022. Antifragile control systems: The case of an oscillator-based network model of urban road traffic dynamics. arXiv preprint arXiv:2210.10460 .

Axenie, C., Kurz, D., Saveriano, M., 2022. Antifragile Control Systems: The Case of an Anti-Symmetric Network Model of the Tumor-Immune-Drug Interactions. Symmetry 14, 2034. doi:10.3390/sym14102034.

Axenie, C., Saveriano, M., 2023. Antifragile Control Systems: The case of mobile robot trajectory tracking in the presence of uncertainty.

Bemporad, A., 2006. Model Predictive Control Design: New Trends and Tools, in: Proceedings of the 45th IEEE Conference on Decision and Control, pp. 6678–6683. doi:10.1109/CDC.2006.377490.

de Bruijn, H., Größler, A., Videira, N., 2020. Antifragility as a design criterion for modelling dynamic systems. Systems Research and Behavioral Science 37, 23–37. doi:10.1002/sres.2574.

Chang, G.L., Xiang, H., 2003. The relationship between congestion levels and accidents URL: https://trid.trb.org/view/680981. number: MD-03-SP 208B46,.

Chen, C., Huang, Y.P., Lam, W.H.K., Pan, T.L., Hsu, S.C., Sumalee, A., Zhong, R.X., 2022. Data efficient reinforcement learning and adaptive optimal perimeter control of network traffic dynamics. Transportation Research Part C: Emerging Technologies 142, 103759. doi:10.1016/j.trc.2022.103759.

Chen, C., Wei, H., Xu, N., Zheng, G., Yang, M., Xiong, Y., Xu, K., Li, Z., 2020. Toward A Thousand Lights: Decentralized Deep Reinforcement Learning for Large-Scale Traffic Signal Control. Proceedings of the AAAI Conference on Artificial Intelligence 34, 3414–3421. doi:10.1609/aaai.v34i04.5744.

Chu, T., Wang, J., Codecà, L., Li, Z., 2020. Multi-Agent Deep Reinforcement Learning for Large-Scale Traffic Signal Control. IEEE Transactions on Intelligent Transportation Systems 21, 1086–1095. doi:10.1109/TITS.2019.2901791.

Daganzo, C.F., 2007. Urban gridlock: Macroscopic modeling and mitigation approaches. Transportation Research Part B: Methodological 41, 49–62. doi:10.1016/j.trb.2006.03.001.

Daganzo, C.F., Geroliminis, N., 2008. An analytical approximation for the macroscopic fundamental diagram of urban traffic. Transportation Research Part B: Methodological 42, 771–781. doi:10.1016/j.trb.2008.06.008.

Darby, M.L., Nikolaou, M., 2012. MPC: Current practice and challenges. Control Engineering Practice 20, 328–342. doi:10.1016/j.conengprac.2011.12.004.

Fang, Y., Sansavini, G., 2017. Emergence of Antifragility by Optimum Postdisruption Restoration Planning of Infrastructure Networks. Journal of Infrastructure Systems 23, 04017024. doi:10.1061/(ASCE)IS.1943-555X.0000380.

Federal Statistical Office, 2020. Mobilität und Verkehr: Panorama (in German/French only). 16704292, Neuchâtel. URL: https://dam-api.bfs.admin.ch/hub/api/dam/assets/16704292/master.

Figueiredo, L., Jesus, I., Machado, J., Ferreira, J., Martins de Carvalho, J., 2001. Towards the development of intelligent transportation systems, in: ITSC 2001. 2001 IEEE Intelligent Transportation Systems. Proceedings (Cat. No.01TH8585), pp. 1206–1211. doi:10.1109/ITSC.2001.948835.

Fu, H., Chen, S., Chen, K., Kouvelas, A., Geroliminis, N., 2022. Perimeter Control and Route Guidance of Multi-Region MFD Systems With Boundary Queues Using Colored Petri Nets. IEEE Transactions on Intelligent Transportation Systems 23, 12977–12999. doi:10.1109/TITS.2021.3119017.

Ganin, A.A., Mersky, A.C., Jin, A.S., Kitsak, M., Keisler, J.M., Linkov, I., 2019. Resilience in Intelligent Transportation Systems (ITS). Transportation Research Part C: Emerging Technologies 100, 318–329. doi:10.1016/j.trc.2019.01.014.

Gayah, V.V., Daganzo, C.F., 2011. Clockwise hysteresis loops in the Macroscopic Fundamental Diagram: An effect of network instability. Transportation Research Part B: Methodological 45, 643–655. doi:10.1016/j.trb.2010.11.006.

Genser, A., Kouvelas, A., 2022. Dynamic optimal congestion pricing in multi-region urban networks by application of a Multi-Layer-Neural network. Transportation Research Part C: Emerging Technologies 134, 103485. doi:10.1016/j.trc.2021.103485.

Geroliminis, N., Daganzo, C.F., 2008. Existence of urban-scale macroscopic fundamental diagrams: Some experimental findings. Transportation Research Part B: Methodological 42, 759–770. doi:10.1016/j.trb.2008.02.002.

Geroliminis, N., Haddad, J., Ramezani, M., 2013. Optimal Perimeter Control for Two Urban Regions With Macroscopic Fundamental Diagrams: A Model Predictive Approach. IEEE Transactions on Intelligent Transportation Systems 14, 348–359. doi:10.1109/TITS.2012.2216877.

Haghighat, A.K., Ravichandra-Mouli, V., Chakraborty, P., Esfandiari, Y., Arabi, S., Sharma, A., 2020. Applications of Deep Learning in Intelligent Transportation Systems. Journal of Big Data Analytics in Transportation 2, 115–145. doi:10.1007/s42421-020-00020-1.

Haque, M.M., Chin, H.C., Debnath, A.K., 2013. Sustainable, safe, smart—three key elements of Singapore's evolving transport policies. Transport Policy 27, 20–31. doi:10.1016/j.tranpol.2012.11.017.

Haydari, A., Yılmaz, Y., 2022. Deep Reinforcement Learning for Intelligent Transportation Systems: A Survey. IEEE Transactions on Intelligent Transportation Systems 23, 11–32. doi:10.1109/TITS.2020.3008612.

Ji, Y., Jiang, R., Chung, E., Zhang, X., 2015. The impact of incidents on macroscopic fundamental diagrams. Proceedings of the Institution of Civil Engineers: Transport 168, 396–405. doi:10.1680/tran.13.00026.

Johnson, J., Gheorghe, A.V., 2013. Antifragility analysis and measurement framework for systems of systems. International Journal of Disaster Risk Science 4, 159–168. doi:10.1007/s13753-013-0017-7.

Kamalahmadi, M., Shekarian, M., Mellat Parast, M., 2022. The impact of flexibility and redundancy on improving supply chain resilience to disruptions. International Journal of Production Research 60, 1992–2020. doi:10.1080/00207543.2021.1883759.

Keyvan-Ekbatani, M., Kouvelas, A., Papamichail, I., Papageorgiou, M., 2012. Exploiting the fundamental diagram of urban networks for feedback-based gating. Transportation Research Part B: Methodological 46, 1393–1403. doi:10.1016/j.trb.2012.06.008.

Kim, H., Muñoz, S., Osuna, P., Gershenson, C., 2020. Antifragility Predicts the Robustness and Evolvability of Biological Networks through Multi-Class Classification with a Convolutional Neural Network. Entropy 22, 986. doi:10.3390/e22090986.

Knoop, V.L., Hoogendoorn, S.P., Van Lint, J.W.C., 2012. Routing Strategies Based on Macroscopic Fundamental Diagram. Transportation Research Record 2315, 1–10. doi:10.3141/2315-01.

Korecki, M., Dailisan, D., Helbing, D., 2023. How Well Do Reinforcement Learning Approaches Cope With Disruptions? The Case of Traffic Signal Control. IEEE Access 11, 36504–36515. doi:10.1109/ACCESS.2023.3266644.

Kouvelas, A., Saeedmanesh, M., Geroliminis, N., 2017. Enhancing model-based feedback perimeter control with data-driven online adaptive optimization. Transportation Research Part B: Methodological 96, 26–45. doi:10.1016/j.trb.2016.10.011.

Li, Y., 2018. Deep Reinforcement Learning: An Overview. ArXiv:1701.07274.

Lillicrap, T.P., Hunt, J.J., Pritzel, A., Heess, N., Erez, T., Tassa, Y., Silver, D., Wierstra, D., 2015. Continuous control with deep reinforcement learning. doi:10.48550/arXiv.1509.02971.

Lucia, S., Tătulea-Codrean, A., Schoppmeyer, C., Engell, S., 2017. Rapid development of modular and sustainable nonlinear model predictive control solutions. Control Engineering Practice 60, 51–62. doi:10.1016/j.conengprac.2016.12.009.

Manso, G., Balsmeier, B., Fleming, L., 2020. Heterogeneous Innovation and the Antifragile Economy .

Mazloumi, E., Currie, G., Rose, G., 2010. Using GPS Data to Gain Insight into Public Transport Travel Time Variability. Journal of Transportation Engineering 136, 623–631. doi:10.1061/(ASCE)TE.1943-5436.0000126.

Mnih, V., Kavukcuoglu, K., Silver, D., Graves, A., Antonoglou, I., Wierstra, D., Riedmiller, M., 2013. Playing Atari with Deep Reinforcement Learning .

Munoz, A., Billsberry, J., Ambrosini, V., 2022. Resilience, robustness, and antifragility: Towards an appreciation of distinct organizational responses to adversity. International Journal of Management Reviews 24, 181–187. doi:10.1111/ijmr.12289.

Mysore, S., Mabsout, B., Mancuso, R., Saenko, K., 2021. Regularizing Action Policies for Smooth Control with Reinforcement Learning, in: 2021 IEEE International Conference on Robotics and Automation (ICRA), pp. 1810–1816. doi:10.1109/ICRA48506.2021.9561138.

Nguyen, H., Kieu, L.M., Wen, T., Cai, C., 2018. Deep learning methods in transportation domain: a review. IET Intelligent Transport Systems 12, 998–1004. doi:10.1049/iet-its.2018.0064.

Ni, W., Cassidy, M.J., 2019. Cordon control with spatially-varying metering rates: A Reinforcement Learning approach. Transportation Research Part C: Emerging Technologies 98, 358–369. doi:10.1016/j.trc.2018.12.007.

Priyadarshini, J., Singh, R.K., Mishra, R., Bag, S., 2022. Investigating the interaction of factors for implementing additive manufacturing to build an antifragile supply chain: TISM-MICMAC approach. Operations Management Research 15, 567–588. doi:10.1007/s12063-022-00259-7.

Qin, S.J., Badgwell, T.A., 2003. A survey of industrial model predictive control technology. Control engineering practice 11, 733–764.

Rodrigues, F., Azevedo, C.L., 2019. Towards Robust Deep Reinforcement Learning for Traffic Signal Control: Demand Surges, Incidents and Sensor Failures, in: 2019 IEEE Intelligent Transportation Systems Conference (ITSC), pp. 3559–3566. doi:10.1109/ITSC.2019.8917451.

Saedi, R., Saeedmanesh, M., Zockaie, A., Saberi, M., Geroliminis, N., Mahmassani, H.S., 2020. Estimating network travel time reliability with network partitioning. Transportation Research Part C: Emerging Technologies 112, 46–61. doi:10.1016/j.trc.2020.01.013.

Silver, D., Lever, G., Heess, N., Degris, T., Wierstra, D., Riedmiller, M., 2014. Deterministic Policy Gradient Algorithms .

Su, Z.C., Chow, A.H.F., Fang, C.L., Liang, E.M., Zhong, R.X., 2023. Hierarchical control for stochastic network traffic with reinforcement learning. Transportation Research Part B: Methodological 167, 196–216. doi:10.1016/j.trb.2022.12.001.

Sutton, R.S., Barto, A.G., 2018. Reinforcement Learning, second edition: An Introduction. MIT Press.

Taleb, N.N., 2012. Antifragile: Things That Gain from Disorder. volume 3. Random House.

Taleb, N.N., 2013. 'Antifragility' as a mathematical idea. Nature 494, 430–430. doi:10.1038/494430e.

Taleb, N.N., Douady, R., 2013. Mathematical definition, mapping, and detection of (anti)fragility. Quantitative Finance 13, 1677–1689. doi:10.1080/14697688.2013.800219.

Taleb, N.N., West, J., 2023. Working with Convex Responses: Antifragility from Finance to Oncology. Entropy 25, 343. doi:10.3390/e25020343.

Tamvakis, P., Xenidis, Y., 2012. Resilience in Transportation Systems. Procedia - Social and Behavioral Sciences 48, 3441–3450. doi:10.1016/j.sbspro.2012.06.1308.

Tan, K.L., Sharma, A., Sarkar, S., 2020. Robust Deep Reinforcement Learning for Traffic Signal Control. Journal of Big Data Analytics in Transportation 2, 263–274. doi:10.1007/s42421-020-00029-6.

Tan, W.J., Zhang, A.N., Cai, W., 2019. A graph-based model to measure structural redundancy for supply chain resilience. International Journal of Production Research 57, 6385–6404. doi:10.1080/00207543.2019.1566666.

Tang, J., Heinimann, H., Han, K., Luo, H., Zhong, B., 2020. Evaluating resilience in urban transportation systems for sustainability: A systems-based Bayesian network model. Transportation Research Part C: Emerging Technologies 121, 102840. doi:10.1016/j.trc.2020.102840.

Vlahogianni, E.I., Karlaftis, M.G., Golias, J.C., 2014. Short-term traffic forecasting: Where we are and where we're going. Transportation Research Part C: Emerging Technologies 43, 3–19. doi:10.1016/j.trc.2014.01.005.

Wang, P., Wada, K., Alamatsu, T., Hara, Y., 2015. An empirical analysis of macroscopic fundamental diagrams for sendai road networks. Interdisciplinary Information Sciences 21, 49–61. doi:10.4036/iis.2015.49.

Wang, Y., Jin, H., Zheng, G., 2022. CTRL: Cooperative Traffic Tolling via Reinforcement Learning, in: Proceedings of the 31st ACM International Conference on Information & Knowledge Management, Association for Computing Machinery, New York, NY, USA. pp. 3545–3554. doi:10.1145/3511808.3557112.

Wei, H., Xu, N., Zhang, H., Zheng, G., Zang, X., Chen, C., Zhang, W., Zhu, Y., Xu, K., Li, Z., 2019. CoLight: Learning Network-level Cooperation for Traffic Signal Control, in: Proceedings of the 28th ACM International Conference on Information and Knowledge Management, ACM, Beijing China. pp. 1913–1922. doi:10.1145/3357384.3357902.

Wu, C., Ma, Z., Kim, I., 2020. Multi-Agent Reinforcement Learning for Traffic Signal Control: Algorithms and Robustness Analysis, in: 2020 IEEE 23rd International Conference on Intelligent Transportation Systems (ITSC), pp. 1–7. doi:10.1109/ITSC45102.2020.9294623.

Wächter, A., Biegler, L.T., 2006. On the implementation of an interior-point filter line-search algorithm for large-scale nonlinear programming. Mathematical Programming 106, 25–57. doi:10.1007/s10107-004-0559-y.

Yang, K., Zheng, N., Menendez, M., 2017. Multi-scale Perimeter Control Approach in a Connected-Vehicle Environment. Transportation Research Procedia 23, 101–120. doi:10.1016/j.trpro.2017.05.007.

Yildirimoglu, M., Ramezani, M., Geroliminis, N., 2015. Equilibrium Analysis and Route Guidance in Large-scale Networks with MFD Dynamics. Transportation Research Procedia 9, 185–204. doi:10.1016/j.trpro.2015.07.011.

Zhang, S., Yao, H., Whiteson, S., 2021. Breaking the Deadly Triad with a Target Network, in: Proceedings of the 38th International Conference on Machine Learning, PMLR. pp. 12621–12631.

Zheng, N., Geroliminis, N., 2016. Modeling and optimization of multimodal urban networks with limited parking and dynamic pricing. Transportation Research Part B: Methodological 83, 36–58. doi:10.1016/j.trb.2015.10.008.

Zheng, N., Waraich, R.A., Axhausen, K.W., Geroliminis, N., 2012. A dynamic cordon pricing scheme combining the Macroscopic Fundamental Diagram and an agent-based traffic model. Transportation Research Part A: Policy and Practice 46, 1291–1303. doi:10.1016/j.tra.2012.05.006.

Zhou, D., Gayah, V.V., 2021. Model-free perimeter metering control for two-region urban networks using deep reinforcement learning. Transportation Research Part C: Emerging Technologies 124, 102949. doi:10.1016/j.trc.2020.102949.

Zhou, D., Gayah, V.V., 2023. Scalable multi-region perimeter metering control for urban networks: A multi-agent deep reinforcement learning approach. Transportation Research Part C: Emerging Technologies 148, 104033. doi:10.1016/j.trc.2023.104033.

Zhou, Y., Wang, J., Yang, H., 2019. Resilience of Transportation Systems: Concepts and Comprehensive Review. IEEE Transactions on Intelligent Transportation Systems 20, 4262–4276. doi:10.1109/TITS.2018.2883766.

Zhu, L., Yu, F.R., Wang, Y., Ning, B., Tang, T., 2019. Big Data Analytics in Intelligent Transportation Systems: A Survey. IEEE Transactions on Intelligent Transportation Systems 20, 383–398. doi:10.1109/TITS.2018.2815678.

Zhu, Y., Wang, P., Corman, F., 2021. A deep reinforcement learning framework for delay management with passenger re-routing, in: 9th International Conference on Railway Operations Modelling and Analysis.